

AGATA PHYSICS CASE



November 2008

Document edited by Dimiter Balabanski and Dorel Bucurescu on behalf of the AGATA collaboration.

The contribution of the following colleagues is gratefully acknowledged:
Giacomo de Angelis, Ayse Atac, Faisal Azaiez, Thomas Aumann, Bertram Blank, Alexander Bürger, Angela Bracco, Bo Cederwall, Dominique Curien, Jerzy Dudek, Enrico Farnea, Martin Freer, Serge Franchoo, Jürgen Gerl, Magne Guttormsen, Gudrun Hagemann, Ikuko Hamamoto, Rolf-Dietmar Herzberg, Jan Jolie, Sotirios Harissopoulos, Herbert Hübel, Rauno Julin, Wolfram Korten, Reiner Krücken, Silvia Leoni, Adam Maj, Witek Meczynski, Daniele Mengoni, Paul Nolan, Johan Nyberg, Robert Page, Norbert Pietralla, Marcello Pignanelli, Dirk Rudolph, Gary Simpson, John Simpson, Olivier Stezowski, Piet Van Duppen, Robert Wadsworth, Phil Walker, Carl Wheldon, Tzanka Wheldon.

CONTENTS

1. Introduction

2. Properties of weakly-bound nuclei far away from stability: nuclear halos, neutron skins, cluster and molecular states

- 2.1. Knock-out reactions
- 2.2. Nuclear clusters and molecular states
- 2.3. Neutron skins

3. Robustness of shell structure far away from stability: magic numbers shell gaps, and shape coexistence

- 3.1. Magic numbers and shell gaps far away from stability
- 3.2. Collectivity of low-lying excited states
- 3.3. Single-particle levels far from stability
- 3.4. Intruder states and many-body effects

4. Isospin degrees of freedom: $N=Z$ nuclei

- 4.1. Neutron-proton pairing
- 4.2. Isospin symmetry

5. Spectroscopy at the proton drip line

6. Collectivity of low-lying excited states. Phase transitions and symmetries in atomic nuclei

7. Exploring the limits of nuclear rotation: extreme nuclear deformations

- 7.1. Superdeformation and hyperdeformation
- 7.2. Jacobi phase transition
- 7.3. Shapes with broken axial symmetry

8. Highly excited states and nuclei at finite temperature

- 8.1. Order-to-chaos transition
- 8.2. Giant resonances
- 8.3. Level densities and gamma-ray strength functions

9. Structure of superheavy nuclei

Appendix 1. Hypernuclei

Appendix 2. Nuclear astrophysics

Appendix 3. Fundamental interactions

Appendix 4. AGATA technical characteristics and simulations

1 Introduction

Modern nuclear physics addresses a number of fundamental questions which determine the priorities of scientific research in our field. A key theme listed in the 2004 NuPECC "Long Range Plan" for nuclear science is:

"what are the forces which act between the nucleons in a nucleus and which arrangements does it take as a result of the interplay between them?"

In more detail, some of the key issues which will need to be resolved include:

- how does nuclear shell structure evolve in exotic neutron-rich nuclei?
- how do collectivity and pairing correlations change in neutron-rich nuclei?
- what is the structure of the heaviest nuclear systems?
- what are the limits of the high-spin domain?

To understand the properties of a nucleus it is not sufficient just to establish the interactions between its components, it is also necessary to determine the arrangements of the nucleons, i.e. the structure of the nucleus. So far our knowledge about the structure of the nuclei has been mostly limited to nuclei close to the valley of beta stability, or nuclei with a deficiency of neutrons, which can be produced in fusion-evaporation reactions with stable beams and stable targets.

To address the basic questions posed above it is necessary to expand nuclear research to exotic nuclei situated far away from the valley of beta stability. A major part of the recent progress in our understanding of the structure of the atomic nuclei is related to the synthesis and study of new species far away from the beta stability line, the development of new experimental methods to study them, as well as the development of new, improved theoretical models of the nucleus.

The accelerators for radioactive ion beams (RIBs), such as the existing REX-ISOLDE, GANIL/SPIRAL and GSI facilities, those under construction such as FAIR, SPIRAL2, and the upgrade of REX-ISOLDE, called HIE-ISOLDE, as well as the future facilities such as SPES and EURISOL, open the possibility to study the structure of nuclei with a large excess of neutrons and give access to a whole new range of experiments on exotic nuclei (which have very different proton-to-neutron ratios compared to stable and near-stable nuclei). In most of the cases these nuclei will be produced in limited quantities and the experiments will be carried out in a high-background environment, which is related to the production process.

The development of a gamma-ray detection system capable of tracking the location of the energy deposited at every gamma-ray interaction point in a detector is a major advance of detector technology which will provide an unparalleled level of detection sensitivity, and will open new avenues for nuclear structure studies. Such an instrument is needed to address the questions listed above and to fully exploit the scientific opportunities at existing and future facilities.

An European collaboration has been established to construct a 4π gamma-ray tracking spectrometer, called AGATA (Advanced Gamma-ray Tracking Array). AGATA will consist of 60 triple-cluster units, each triple-cluster unit being an assembly of three 36-fold segmented Ge detectors. A first implementation of 5 AGATA units, the so-called demonstrator, which is currently being assembled, will already provide a significant gain in sensitivity for a large number of experiments with fast and ISOL, or post-accelerated ISOL

RIBs, as well as with intense stable beams. Many of these experiments will involve studies using "inverse kinematics" where beams of exotic nuclei near the drip line, produced from fission or fragmentation at relativistic energies, are investigated. For these experiments a highly segmented detector able to track the gamma-ray interactions is needed to minimize Doppler effects.

This document presents subjects of actual interest in nuclear structure physics, which will consistently benefit from the use of the AGATA array. It is, nevertheless, fair to emphasize that, with the new RIB facilities at the promised performances, some of the important contributions of AGATA to the atomic nucleus structure physics will constitute surprising discoveries.

2 Properties of weakly-bound nuclei far away from stability: nuclear halos, neutron skins, cluster and molecular states

2.1 Knock-out reactions: Spectroscopic studies of halo nuclei and nuclei away of stability

When one deals with light mass nuclei with a very different proton-to-neutron ratio as compared to stable nuclei, a natural question arises: *how does binding energy and extreme proton-to-neutron asymmetries affect nuclear properties?*

The appearance of the nuclear halo coincides with two important characteristics, the weak binding of the valence nucleons and the occupancy of low angular momentum orbits (for which the centrifugal barrier is suppressed). The characteristic lowering of the $2s$ orbit from the sd -shell such that it competes with p -orbits from the $1p$ shell is considered to be the reason for the appearance of a halo structure in the ground state of ^{11}Be .

The properties of a quantal system are fully described by means of its wave function. The measurement of the momentum distribution of particles emitted in knock-out reactions is one of the techniques to study the wave functions of nuclei far away from stability, as well as halo nuclei. A strong limitation of this technique is so far related to the fact that the residual nucleus has a variety of excited states. The utilization of a high-resolution, highly efficient detector to identify and classify the final states will provide a breakthrough in these studies, especially in cases when the number of excited states is large (as shown as an example in Fig. 2.1.1).

2.2 Nuclear clusters and molecular states

Gamma-ray spectroscopy far from stability is a difficult task because the production cross-sections are low and there is a high background. The current state-of-the-art experiments address studies at the proton drip line (see Section 4), but the future major challenges are when approaching the neutron drip line.

At the neutron drip line the neutrons are extremely weakly bound. It is suggested that many nuclei close to this limit can be described as having a component of a relatively inert cluster core embedded within a sea of valence neutrons. The valence neutrons would be shared, or exchanged between the cores, and as such the nucleus can be described as a nuclear molecule. Such states are the analogs of those found in atomic molecules which result from the covalent exchange of electrons [2.2]. In order to prove the nature of such states, the electromagnetic transitions between members of the associated rotational bands, or alternatively, their decay to low-lying normal states, need to be measured. As an

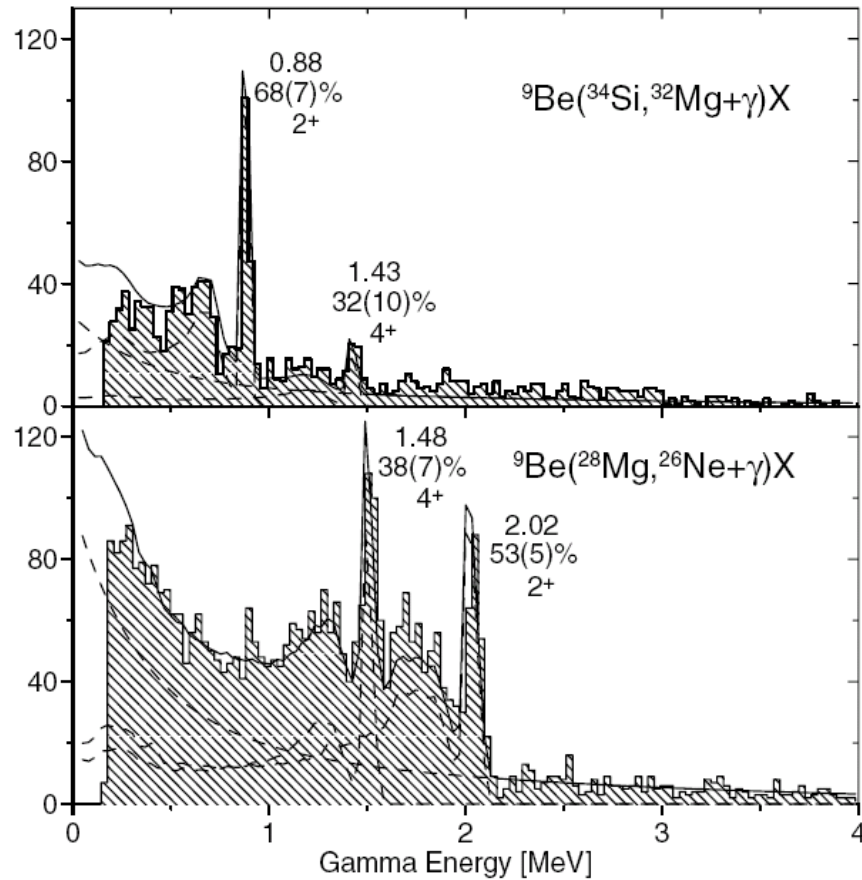


Figure 2.1.1. Gamma-ray spectra (SeGA array) for two-proton removal reactions at 82 MeV/A (Ref. [2.1]).

example, the 0^+ , 6.18 MeV excited state in ^{10}Be has a measurable gamma-decay branch to the ground state, and the isomeric nature of this transition is linked to its developed molecular structure. The search for such states has already been carried out with existing instruments, but a breakthrough is expected to happen with the AGATA detector due to its superior resolution and selectivity. Figure 2.2.1 shows the series of electromagnetic transitions investigated to date in the beryllium isotopes. Important advances will be in determining the structural properties of three-centre systems in the carbon isotopes, in making the step from our understanding of nuclear dimers to nuclear polymers.

2.3 Neutron skins

In stable nuclei, the strong proton-neutron interaction keeps the volumes occupied by protons and neutrons almost identical. This is no longer the case in nuclei with large neutron excess. The surface region is predominantly occupied by neutrons, which form a skin-like structure. Those nuclei are characterized not only by a very great spatial extension but also by a weaker binding energy of the last nucleons, compared to the much higher density in the interior. The neutron skin thickness is predicted to be up to 1 fm. This would mean, e.g., for the Sn nuclei, that the strongly neutron-enriched outer zone comprises up to half of the entire nuclear volume. Within this surface zone,

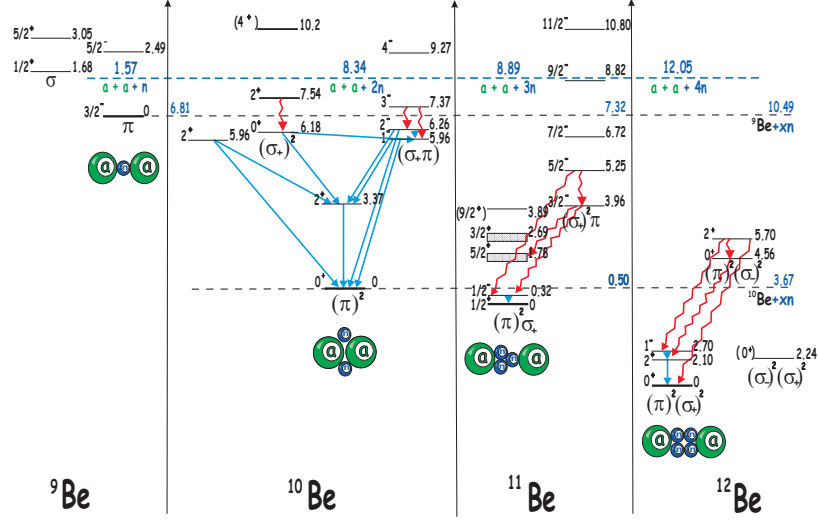


Figure 2.2.1. Electromagnetic transitions investigated in the beryllium isotopes. The schematic Ikeda diagram (Ref. [2.2]) shows the $2\alpha +$ valence neutron structures and the types of orbitals (σ – and π – bond) in which the neutrons reside. The blue and red arrows are the observed and possible (unobserved) gamma-ray transitions, respectively (Tz. Kokalova, Ph.D thesis, Freie Universität Berlin, 2003).

the composition of the nuclear medium approaches that of the neutron matter with an average density significantly below that of nuclei. Evidently, this provides an ideal case for probing isospin and density dependence of the nuclear force.

An important feature of this region is that it will shed light on the structure of nuclei along the r -process path, the route through which about half of the heavy elements have been synthesized.

The impact of the skin of neutrons on the rotation of the core can be studied in detail by observation of the high-spin states in these nuclei. This can be done by utilizing the deep inelastic reactions. Such experiments will take advantage of the high granularity and the tracking possibilities of AGATA in combination with a recoil spectrometer for identification of the reaction path.

References

- [2.1] D. Basin *et al.*, Phys. Rev. Lett. 91(2001)012501.
- [2.2] K. Ikeda, Suppl. Progr. Theor. Phys. (Japan), extra number 464(1968).

3 Robustness of the shell structure away from stability: magic numbers, shell gaps and shape coexistence

The nuclear shell model as we know it nowadays reflects our understanding of the structure of nuclei lying close to the stability line. The atomic nucleus, being a many-fermion system, is described in the approximation of almost independent particles that move in a common potential. This approximation results in a single-particle shell structure of the nucleus. Characteristic shell gaps appear in the single-particle spectrum of protons and

neutrons and are the cause for the so-called *magic numbers*. For these particle numbers the single-particle shells are filled. These nuclei have increased particle stability, spherical (for doubly-magic nuclei) or near-spherical shape (when the shell is filled for only one species). It should be noted, however, that the parameterization of the nuclear potential also reflects the properties of stable nuclei.

New phenomena are predicted close to the neutron drip line where the binding energies for the last occupied neutrons approach zero. Mean-field calculations suggest that the nuclear potentials will diverge from those encountered close to stability. This could lead to a change in the single-particle orbit ordering. As a result, changes in the shell gaps can occur which may produce changes of the magic numbers away from stability.

3.1 Magic numbers and shell gaps far away from stability

The evolution of shell structure in neutron-rich nuclei reflects the spin and the isospin dependence of the in-medium nucleon-nucleon interaction. In contrast with stable nuclei, where a strong proton-neutron interaction is a key ingredient to induce deformation of the whole nucleus, decoupling between valence neutrons and the core could occur in very neutron-rich nuclei. Decoupling, or strong polarization effects in nuclei could be searched for by measuring the electric quadrupole strength, $B(E2)$, which is sensitive to the proton contribution of the excitation, along a singly-magic isotopic chain. In particular, Coulomb excitation experiments give access to the energy of the first 2^+ state and the associated $B(E2)$ transition rate in even-even nuclei. When such data are systematically analyzed as a function of the proton and neutron numbers, changes of shell gaps and shifts of the magic gaps can be localized. The cause of these changes is the orbit dependent interactions between neutrons and protons. Because orbits far away of stability can now be filled strong effects due to the so-called $\tau\sigma$ interaction [3.1] are observed. An example of such interaction has been observed around ^{32}Mg , known as the "island of inversion". Measurements of reduced transition probabilities $B(E2)$ in this case help to understand the degree of mixing.

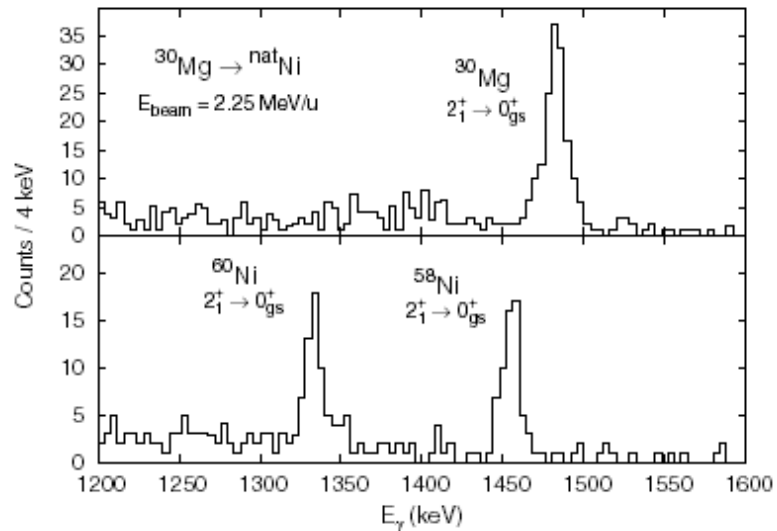


Figure 3.1.1. Coulomb excitation spectra from the Mg region (Ref. [3.2]).

First experiments, using Coulomb excitation of radioactive beams were done utilizing fast and ISOL beams with present instruments (see Fig. 3.1.1. for experimental results obtained with the Miniball spectrometer at REX-ISOLDE in CERN). The increased segmentation of AGATA will allow to perform these experiments farther from stability.

3.2 Collectivity of low-lying excited states

An important aspect in the understanding of the structure of nuclei very far away from stability is to track the evolution of collective excitations with proton and neutron number. One of the excited modes of interest are the low-lying vibrational states near closed-shell nuclei. Fig. 3.2.1. shows as an example the onset of collectivity in the Sn isotopes, when one moves away from the closed shell. A comparison with shell model calculations shows that a larger effective charge is needed to reproduce the experimental $B(E2)$ values compared to higher mass Sn isotopes, indicating a greater core polarization due to particle-hole excitations. One can also see that the observed asymmetry of the measured $B(E2)$ values with respect to the middle of the shell requires further theoretical developments.

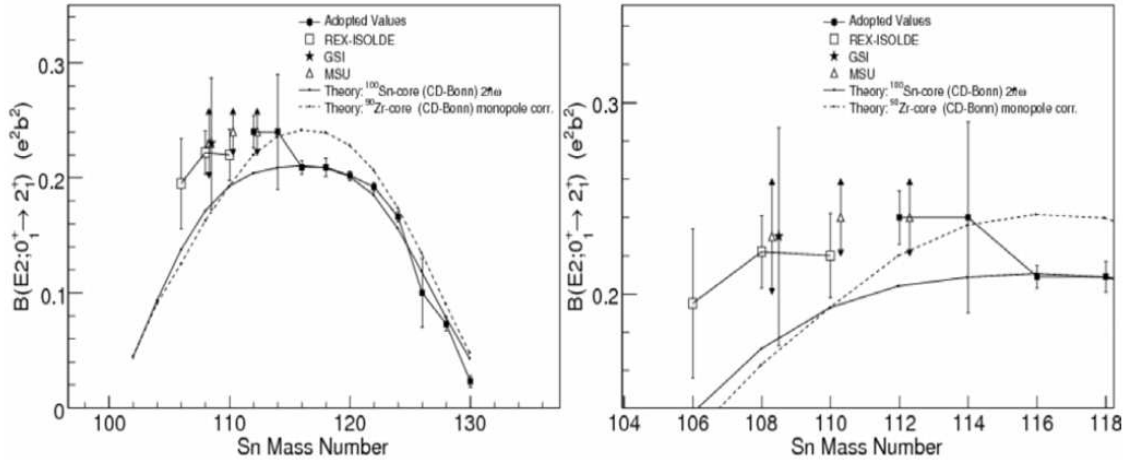


Figure 3.2.1. Experimental and theoretical $B(E2)$ strengths for Sn isotopes [3.3,3.4,3.5]. The curves represent predictions of shell model calculations (dashed curve: using ^{100}Sn as a core, and a $\nu(g_{7/2}, d, s, h_{11/2})$ model space with a neutron effective charge $e_{eff}^\nu = 1.0e$; solid line: ^{90}Zr core and a $\pi(g, d, s)\nu(g_{7/2}, d, s, h_{11/2})$ model space with $e_{eff}^\nu = 0.5e$).

Higher spin states can provide additional important information on the physics of neutron-rich nuclei. For example, in even-even collective nuclei the ratio of the 4^+ to the 2^+ energy, $R_{4/2}$, gives a clear indication on whether the nuclei are rotational ($R_{4/2} = 3.33$), or vibrational ($R_{4/2} = 2$). One of the most intriguing questions related to the properties of nuclei near the neutron drip-line is whether the extended neutron distribution could produce new collective modes in which protons and neutrons exhibit different motions. For example, if the neutron skin rotates, but the core makes no contribution, the observation of excited states related to this mode will provide information about the neutron-neutron correlations within the surface region. Intriguing evidence of this kind was claimed for ^{16}C [3.6], but a more precise recent measurement of the lifetime of the first excited 2^+ state does not support an interpretation with valence neutrons decoupled from the core [3.7].

Another important way to understand collective excitations in atomic nuclei is through measurements of electromagnetic moments. Nuclear magnetic moments are sensitive to the orbits occupied by the valence particles, while electric quadrupole moments probe the deformation and the collective behavior of nuclei at both low and high excitation energy. Generally, the magnetic moments probe 1p-1h excitations across a magic shell gap whereas quadrupole moments are sensitive to quadrupole particle-core coupling interactions (2p-2h excitations). Both, the nuclear gyromagnetic factor and the electric quadrupole moment can be compared to theory and thus play an important role in disentangling the nuclear shell structure far away from stability. Measurements of electromagnetic moments of low-lying states (through Coulomb excitation or transient-field techniques), as well as of isomeric states in nuclei far from stability will be done around a secondary target station in "in-beam" experiments either with fast beams, or with post-accelerated ISOL beams. A large variety of techniques have been developed and used in different laboratories. In general, in these experiments, the radiation emitted at the target position is detected and the AGATA detectors would substantially increase the sensitivity and the detection efficiency for this important class of experiments.

3.3 Single-particle levels far from stability

Single-particle and pairing degrees of freedom play a central role in understanding the structure and the properties of atomic nuclei. With increasing proton/neutron excess one expects modifications of the nuclear mean-field potentials, which in turn modify the position of the single-particle levels. For example, changes of the diffuseness of the nuclear potential might cause a gradual migration of single-particle levels, which may even cross within one major shell. Such an effect has been observed and is extensively studied nowadays around the singly-magic ^{68}Ni , where an inversion of the $1f_{5/2}$ and $2p_{3/2}$ orbits is predicted to occur in the region between ^{75}Cu and ^{79}Cu (see Fig. 3.3.1).

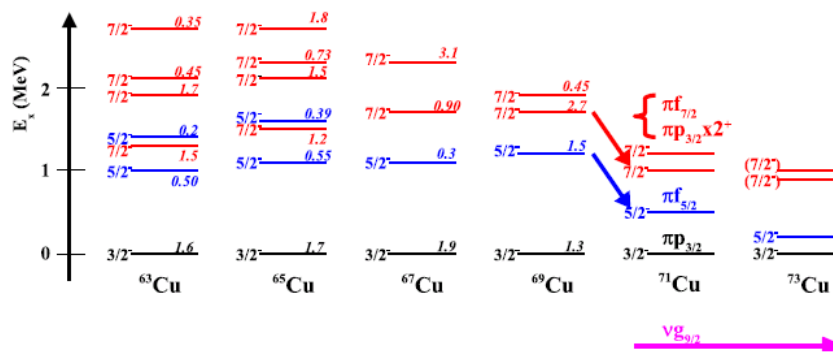


Figure 3.3.1. Level systematics in Cu isotopes [3.8, 3.9].

It is unclear at present what is causing these changes in single-particle orbitals. Changes in the mean-field itself or specific aspects of the residual proton-neutron interactions have been suggested. Away from the valley of stability, changes of spin-orbit strength may occur. This is due to the increase of the surface diffuseness which may lead to a decrease of the spin-orbit interaction. This means that orbits of the same parity (i.e. resulting from a shell with the same principal quantum number) tend to group together. When approaching the neutron drip-line the shell structure of nuclei will be considerably changed

due to the fact that the major part of the weakly-bound neutron wave functions with low- ℓ values can extend to the outside part of the finite potential. The suggested (and partially observed) new magic numbers are $N=16$ and 34 , while those with $N=8$ and 20 disappear. New magic numbers like $N = 40$ or 70 could also appear. The above mentioned migration of single-particle levels will be a subject of active research especially with the expected availability of intense and pure RIBs at different energies. The new detection setups that will be developed for these studies benefit significantly from an instrument such as AGATA. While single-nucleon transfer reactions are the most direct and unambiguous probe of single-particle structure, pair transfer is a direct and unambiguous probe of pairing correlations. Changes of shell structure in nuclei away from stability will be manifested by large changes in single-nucleon and pair transfer cross sections to individual nuclear states. For example, valence single particle orbits can be probed by studying single-particle transfer reactions with radioactive beams. Used in combination with an ion-detection system, AGATA will provide the needed sensitivity to measure the transfer angular momentum and spectroscopic factor to individual states in nuclei far from stability. Utilization of polarized targets will enable the experimental measurement of analyzing power, yielding the orbital quantum number, ℓ . In general, studies of transfer with radioactive heavy ions will simultaneously probe the interplay of single-particle, pairing, and collective degrees of freedom. Isomeric states are typically associated with shell closures, and the isomerism will give valuable additional selectivity for studying the most exotic nuclei. Indeed, a radioactive beam might specifically be selected to be in an isomeric state.

The study of the single-particle structure far away from stability benefits also from measurements of the gyromagnetic factors of the excited states. As emphasized in the previous chapter, they are sensitive to the orbits occupied by the valence particles. Also, the g -factors of the 2^+ states provide a direct estimate of the collective part of this quantity.

3.4 Intruder states and many-body effects

Collective rotational and vibrational degrees of freedom are a dominant feature of nuclear structure. Studies of co-existence of states with very different collectivity in individual nuclei, as well as the evolution of the collective correlations with proton and neutron numbers helps to understand the deformation driving forces of different quasiparticle excitations. In a deformed mean field, energies of high- j orbits strongly depend on the deformation. By exciting particles across the magic gap into deformation-driving states, one obtains deformed intruder configurations that are observed in various regions of the nuclear chart. Studies of such states are very interesting for evaluating the sizes of shell gaps in different parts of the chart of nuclei and especially away from stability. The energies of such intruder configurations depend on the initial position of a high- j orbital at spherical shape, but also on the strength of the quadrupole-quadrupole component of the nuclear interaction and its interplay with pairing which acts towards restoring the spherical symmetry. For example, in nuclei near the $N = 104$ mid-shell of the Pb region, oblate and prolate minima coexist with the nearly spherical ground state at low energy. These intruder deformed structures are associated with multi-proton excitations across the $Z = 82$ gap similarly to those in the ^{32}Mg region (Ch. 3.1). Fig. 3.4.1 demonstrates how the competition of these shapes rapidly changes level patterns in the yrast line of even- A Pb isotopes when approaching the neutron midshell. In ^{186}Pb the first three lowest-lying states are 0^+ states with different deformations. To understand the evolution of these shapes and their mixing, high-efficiency gamma-ray spectrometer is needed in Recoil-Decay-Tagging measurements

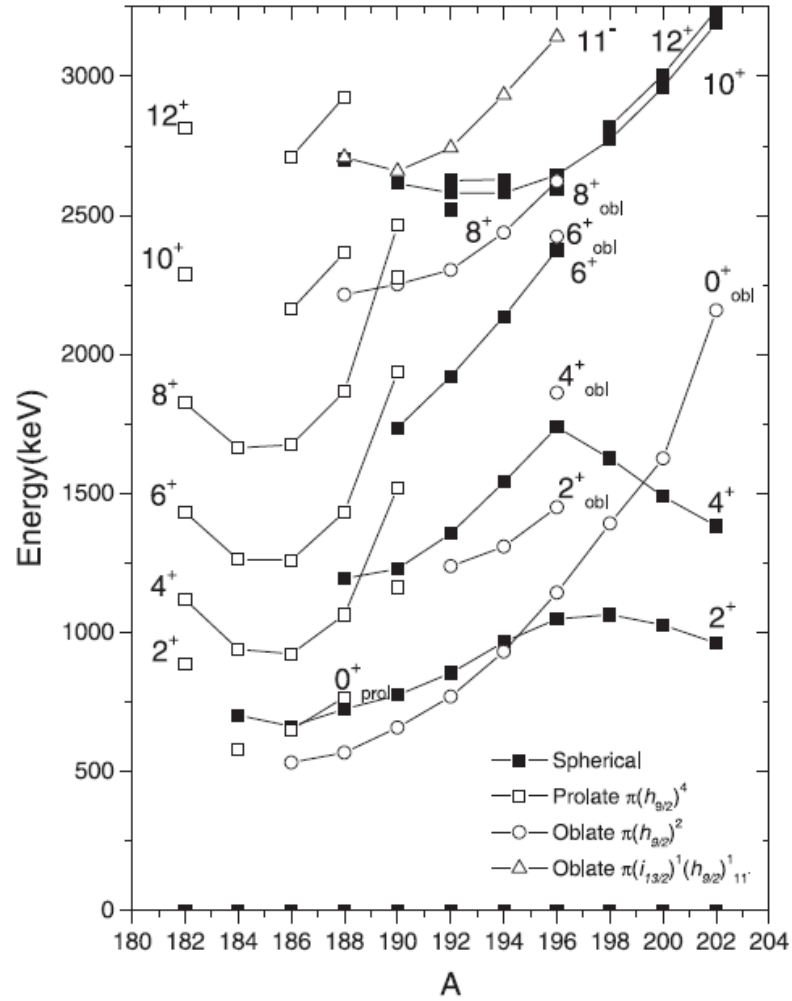


Figure 3.4.1. Systematics of energy levels in neutron-deficient even-A Pb nuclei [3.10].

to obtain more detailed information about the non-yrast states.

References

- [3.1] T. Otsuka *et al.*, Phys. Rev. Lett. 87(2001)082502.
- [3.2] O. Niedermeyer *et al.*, Phys. Rev. Lett. 94(2005)172501.
- [3.3] A. Ekström *et al.*, Phys. Scr. T125(2006)90.
- [3.4] J. Cederkäll *et al.*, Phys. Rev. Lett. 98(2007)172501.
- [3.5] A. Ekström *et al.*, Phys. Rev. Lett. 101(2008)012502.
- [3.6] Z. Elekes *et al.*, Phys. Lett. B586(2004)34.
- [3.7] M. Wiedeking *et al.*, Phys. Rev. Lett. 100(2008)152501.
- [3.8] S. Franchoo *et al.*, Phys. Rev. Lett. 81(1998)3100.
- [3.9] I. Stefănescu *et al.*, Phys. Rev. Lett. 100(2008)112502.
- [3.10] R. Julin *et al.*, J. Phys. G27(2001)R109.

4 Isospin degrees of freedom: $N=Z$ nuclei

Nuclei along the $N=Z$ line and close to it display unique characteristics that arise from two principal sources. First, the neutrons and protons occupy the same orbitals and have maximum spatial overlap of their wave functions, which leads to the development of strong collective effects when the number of valence nucleons increases. The second is that the charge-independence of the nuclear force gives rise to a neutron-proton symmetry (represented by the isospin quantum number), which manifests itself in some structure features observable only on, or very near, the $N=Z$ line.

4.1 Neutron-proton pairing

A phenomenon expected to manifest itself most strongly in the heavier $N=Z$ nuclei, is the neutron-proton pairing, which is a new kind of superfluidity of nuclear matter. In nuclei far away from $N=Z$, the proton-proton (pp) and neutron-neutron (nn) pairing dominate, whereas in nuclei with $N\approx Z$ a sizable contribution of neutron-proton (np) correlations is expected due to the strong overlap of the wave functions. These correlations can be isovector ($T=1, S=0$) or isoscalar ($T=0, S=1$). Figuring out their character and whether they form a static pair condensate (an average field, made of np Cooper pairs) has been a continuous challenge since medium mass $N=Z$ nuclei came into the reach of experiments. The isovector np pairing is mostly clarified. The comparison of theory with existing experimental data indicates a strong isovector np pair field at low spins, whose strength is defined by the isospin symmetry. At higher spins, it is destroyed. On the other hand, it is still an issue of debate whether the *isoscalar np pair correlations lead to a pairing condensate*; also, its strength is still to be determined from appropriate experimental data. Isoscalar np pairing may play a role in the beta-decay, double beta-decay, transfer reactions, or alpha decay, but important clarification is expected from the gamma-ray spectroscopy of the $N\approx Z$ nuclei. The isoscalar np pair has aligned spins, therefore it is expected to be more robust against rotation than the isovector one, which is rapidly quenched by increasing rotation frequency. Thus, if the isoscalar pairing exists and has a reasonable strength, one expects to observe anomalies in the particle alignments (or breaking of nucleon pairs), that is, either the absence, or a delay in the rotational frequency at which such pairs break in the even-even $N=Z$ nuclei, compared to the heavier mass isotopes. Such a delay has been indeed systematically observed in the $N=Z$ even-even nuclei above ^{72}Kr , and it may be an indication of the formation of the isoscalar pair condensate (Fig. 4.1.1).

The current theoretical interpretation of the existing experimental data does not exclude the possibility of the existence of the $T=0$ pairing condensate. Such expected delay in alignment is absent in ^{68}Se and in ^{72}Kr . In ^{72}Kr , one of the best studied cases, there is some evidence of strong mixing of configurations that may be related between them by the transfer of a $T=0$ np pair, but recent measurements of electromagnetic transition probabilities [4.2] indicated no need to consider such a pairing field. High spin configurations possibly related by the transfer of a $T=0$ np pair have also been observed in ^{73}Kr [4.3]. Here the negative parity bands show evidence for an unusual type of band crossing which cannot be explained within standard mean field calculations and also indicate unusually strong configuration mixing. Whether or not this configuration mixing can be accounted for within mean field theory including $T=0$ np pairing is presently under study. For other, heavier nuclei, the experimental data are rather insufficient. The investigation of the yrast

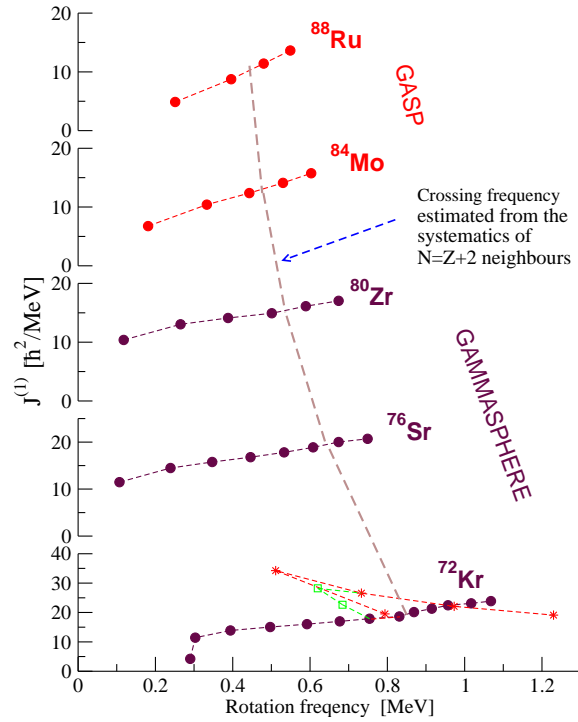


Figure 4.1.1. Delayed alignment in the heavy $N=Z$ nuclei, a possible effect of the np pairing (from Ref. [4.1]).

sequence of the even-even nuclei through the angular momentum region of the expected pair breakings, as well as the investigation of the excited states in $N=Z$ odd-odd nuclei, in the region above mass 80, are expected to bring a decisive contribution to the elucidation of the np pairing issue. More detailed studies of the heavier odd-mass nuclei with $N=Z+1$ (observation of bands with different single-particle origins, and at higher spins) may also provide helpful data in this respect. However, extending these investigations in the exotic region close to ^{100}Sn requires γ -ray spectroscopy with unprecedented sensitivity and efficiency, like AGATA.

4.2 Isospin symmetry

The isospin symmetry leads to the concepts of isobaric multiplets and mirror nuclei, whose structure differs only because of the Coulomb force. The increase in sensitivity and resolving power of the gamma arrays have allowed during the last decade more and more detailed studies of mirror energy differences, that is, differences in the excitation energies at each yrast state of mirror nuclei (and in isobaric multiplets).

These differences give information on the nucleon alignment at the backbending, the evolution of the nuclear radii along the bands, as well as on the configuration of the states. Finally, this allows figuring out the interplay between the Coulomb potential and possible isospin-breaking nuclear interaction terms. Such studies have been performed mainly in medium-light nuclei (see, as an example, Fig. 4.2.1). Extension to other regions (higher masses) are planned, since it is important to determine the limit of the validity of the isospin symmetry with increasing mass; look for isospin non-conserving terms of the

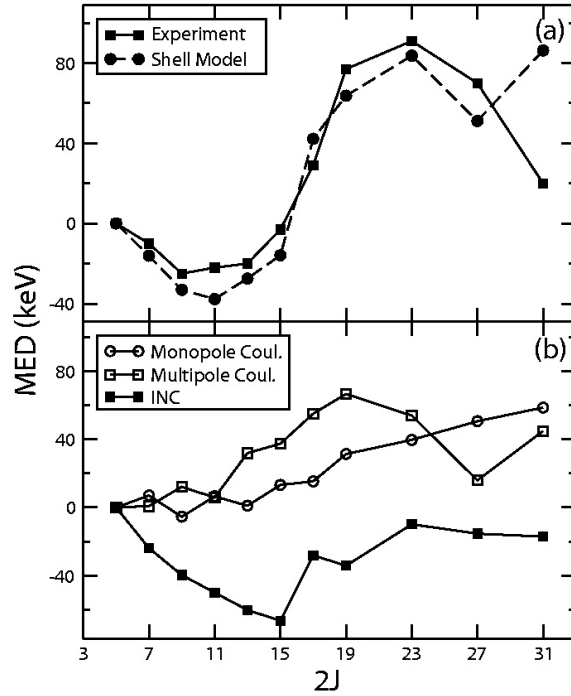


Figure 4.2.1. Mirror energy differences (MED) for the isobaric states in the g.s. rotational band in ^{49}Mn - ^{49}Cr . a) comparison with shell model calculations; b) different terms entering the calculations (from [4.4]).

nuclear interactions; identify the origins of the symmetry breaking; eventually find new Coulomb effects. Measuring isospin multiplets means exploring nuclei on both sides of $N=Z$ line, which, with increasing mass becomes a very difficult task without an array of very high efficiency.

Electromagnetic transition probabilities are also crucial probes of the isospin symmetry, and its validity with increasing values of A and Z . Such determinations require still higher experimental sensitivities. If the isospin symmetry is valid, there are two important consequences: E1 ($\Delta T=0$) transitions in $N=Z$ nuclei are strictly forbidden, and E1 transitions in mirror nuclei must have equal strengths. The isospin symmetry is mainly broken by the Coulomb interaction. It is important to understand the mechanism of the isospin mixing in nuclei since this is used in the determination of the coupling constant from $\log ft$ values of superallowed Fermi decays, and may be also related to unitarity tests of the CKM matrix. A possible way to study the isospin symmetry breaking is to observe experimental deviations from the two rules above.

Observation of isospin forbidden E1 gamma transitions in the even-even $N=Z$ nuclei, as well as differences in E1 transitions in mirror nuclei may be used to determine the origins of the isospin symmetry breaking, which can be due to: isospin breaking of the nuclear interactions; isospin mixing due to coupling to the continuum; isospin mixing of quasi-degenerate levels with the same J^π and different T ; isospin mixing with the isovector giant magnetic resonance. Theoretical estimates, mainly limited to the ground state of even-even nuclei, show that the amount of isospin mixing increases with the mass number A , and, for given A , is maximum at $N=Z$. Forbidden E1 transitions have been observed

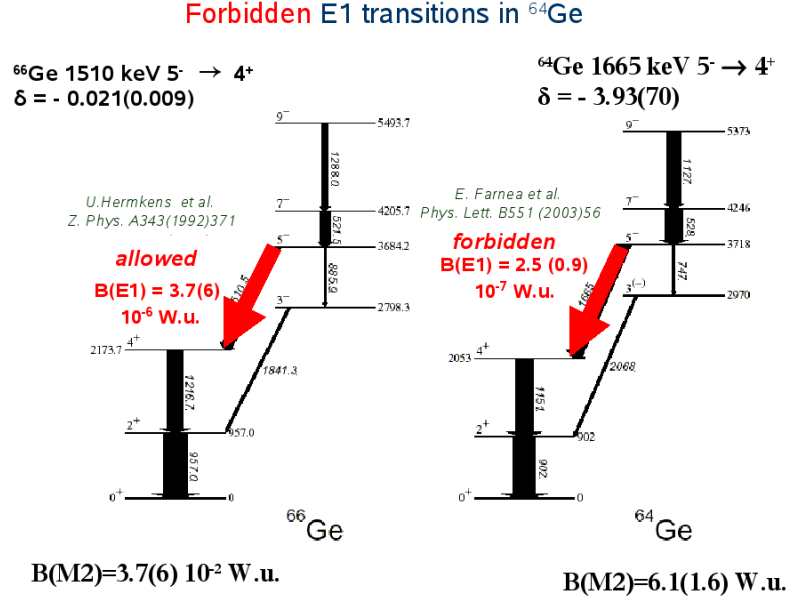


Figure 4.2.2. Forbidden E1 transition measured in the $N=Z$ nucleus ^{64}Ge [4.5].

until now only in the even-even nuclei ^{48}Cr and ^{64}Ge , in the later (ref. [4.5], see also Fig. 4.2.2) the estimated minimum isospin mixing being 2.3 ± 1.4 %, Irregular transitions have been observed in pairs of light mirrors, like ^{35}Ar - ^{35}Cl [4.6]. Such investigations are only at the beginning.

The advance on the $N=Z$ line has led until now to the experimental observation of ^{100}Sn and some limited gamma-ray spectroscopy of several nuclei with mass above mass 80: the heaviest even-even nucleus for which excited states are known is ^{88}Ru [4.7], while the heaviest odd-odd nuclei ^{92}Nb and ^{96}Tc were recently studied at GSI through isomeric decays [4.8]. Heavier $N=Z$ nuclei, as well as those with $T_z = -1$, are very difficult to study. In fusion-evaporation reactions with stable targets/beams, they are produced with very low cross sections (e.g., less than $10 \mu\text{b}$ for ^{88}Ru) and the existing results have exhausted the sensitivity of the present gamma-ray arrays (GAMMASPHERE, EUROBALL, GASP), so that the continuation of such studies clearly requires much higher performances in the gamma detection. The use of fusion-evaporation or direct reactions with radioactive ion beams will increase the possibilities of investigating $N \approx Z$ nuclei at higher masses, spin and isospin. In such cases the use of a gamma-ray detector array with high granularity and efficiency like AGATA, and of efficient particle detectors, will be essential.

References

- [4.1] D. Bucurescu, Acta Phys. Polonica 38(2007)1331.
- [4.2] C. Andreoiu *et al.*, Phys. Rev. C75(2007)041301.
- [4.3] N.S. Kelsall *et al.*, Phys. Rev. C65(2002)044331.
- [4.4] A.P. Zuker *et al.*, Phys. Rev. Lett. 89(2002)142502.
- [4.5] E. Farnea *et al.*, Phys. Lett. B551(2003)56.
- [4.6] F. della Vedova *et al.*, Phys. Rev. C75(2007)034317.

- [4.7] N. Mărginean *et al.*, Phys. Rev.C63(2001)031303R.
 [4.8] A.B. Garnsworthy *et al.*, Phys. Lett. B660(2008)326.

5 Spectroscopy at the proton drip line

Studies of the nuclei along the proton drip line are possible either with radioactive beams, or with intense stable beams. With the advent of new radioactive beam facilities, there will be the opportunity to reach nearly all elements. Near ^{100}Sn , the proton drip line is close to the $N=Z$ line and some interesting physics questions have already been discussed in ch. 4. One of the most interesting directions of study at the proton drip line is the *proton radioactivity*. The proton emission from such nuclei is slowed down by the repulsive Coulomb interaction (which, on the other hand, pushes the drip line closer to stability in comparison with the neutron drip line). Proton decay, with observed lifetimes ranging from hundreds of milliseconds down to femtoseconds, is governed by the quantum tunnelling through the Coulomb barrier; thus, one can study even nuclei that lie beyond the drip line, having quasi-bound protons. Future studies will open the opportunity to

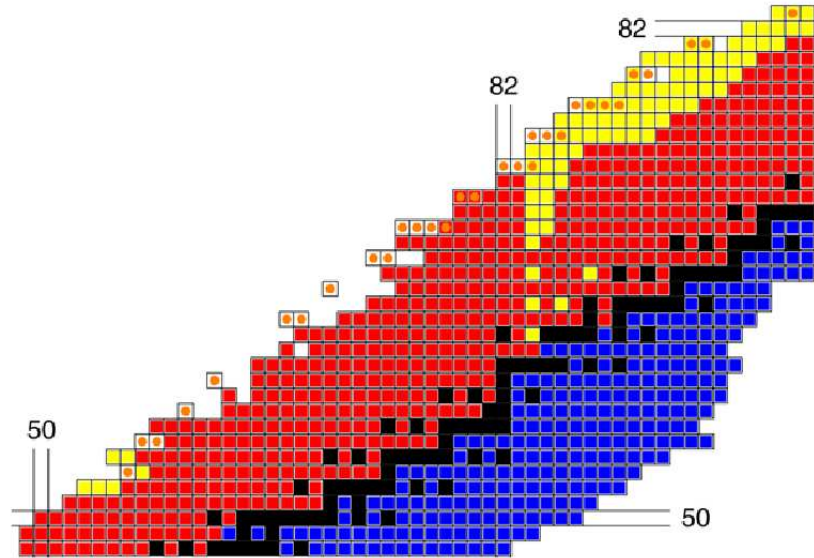


Figure 5.1.1. Proton emitters (marked by orange circles) in the nuclear region between $Z = 53$ and 83 (Ref. [5.1]).

study the expected smooth transition towards the continuum, where the protons are in the particle continuum, which will become more and more accessible in the future for nuclei beyond $A=20$ or so. The structural information that can be obtained from the observed decay pattern and rates concerns the quantum numbers and structure of the parent and daughter states, as well as the effective interactions, pairing, and nuclear shape in these exotic nuclear regions. In some regions of heavy nuclei the parent nuclei are not spherical, which gives a unique possibility to study tunnelling through a three-dimensional barrier.

Proton radioactivity investigations will benefit from the association with γ -ray spectroscopy, usually in the recoil decay tagging or proton-gamma tagged prompt spectroscopy. The prospect of finding new cases of proton emission from high-lying states, competing

with the "prompt" gamma-decay (one such case has been found, ^{58}Cu , see Ref. [5.2]) is also very exciting, as well as proton emission from high-spin isomers. Fragmentation beam spectroscopy (at GSI for example) with AGATA and an efficient particle ball will be one of the main ways of approach. With new radioactive beams and powerful gamma-detection techniques, the nuclear structure near and beyond the proton drip line can be systematically studied. In this region will be encountered cases of doubly magic nuclei, like ^{48}Ni , ^{56}Ni , ^{100}Sn , and their spectroscopy is a unique opportunity to study the robustness of these new combinations of the classical neutron and proton magic numbers.

References

- [5.1] B. Blank, M.J. Borge, *Progr. Part. Nucl. Phys.* 60(2008)403
 [5.2] D. Rudolph *et al.*, *Phys. Rev. C* 63(2000)021301(R)

6 Phase transitions and symmetries in atomic nuclei

Mapping the evolution of nuclear collectivity with the onset of deformation and the different changes in nuclear shapes, is a very challenging task. The geometric models comprise three idealized regimes that describe collective nuclear motion: the anharmonic vibrator, the symmetrically deformed rotor (prolate or oblate), and the triaxial rotor, each one associated with a particular nuclear shape: spherical, axial-ellipsoidal, and triaxial-ellipsoidal. On the other hand, in the interacting boson model, the three geometric limits correspond to three *dynamical symmetries*: U(5), SU(3), and O(6), respectively. The way the nuclear structure changes from one symmetry to another, when the number of valence nucleons is varied, is one of the most interesting questions. It was found that, although nuclei have a limited number of constituents, the transitions between the different limits have a phase transitional character, passing through critical points which are approximately realised in atomic nuclei. The transitions are of first order between spherical and deformed shapes and of second order between oblate and prolate deformation. Where both phase transitions touch each other the phase transition forms a triple point that can be described by Landau's theory of continuous phase transitions [6.1]. These critical shape/phase transi-

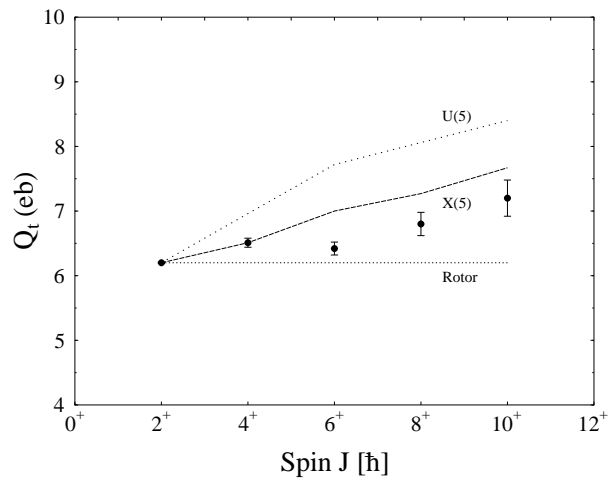


Figure 6.1. Transition quadrupole moments for the yrast band in ^{154}Gd compared to those for a spherical vibrator, deformed rotor and the X(5) prediction [6.2].

tions have been described analytically by introducing new symmetries which correspond to a phase transition when going from the vibrational to the rotational limit, denoted as X(5) [6.3], or to the transition from the vibrational to the γ -soft limit, denoted as E(5) [6.4]. For these symmetries parameter-free analytical expressions were obtained for both energies and reduced electromagnetic transition probabilities. Empirical realizations were found for X(5) in some nuclei around $A=180$ and in the $N=90$ isotones between Nd and Er (see, e.g., Fig. 6.1.), while the E(5) symmetry was suggested in ^{134}Ba and the light Ru, Pd isotopes [6.5].

Transition probabilities between different low-lying non-yrast states are very important fingerprints for critical point symmetries. The mapping of the shape/phase transitions was limited so far to neutron-deficient nuclei close to the stability line for which detailed knowledge on transition rates existed. It will be necessary and needed to extend these studies towards nuclei far from stability, as well as to study the existing candidates for critical-point nuclei in much more detail. Obviously, such studies will benefit from a superior gamma-array like AGATA.

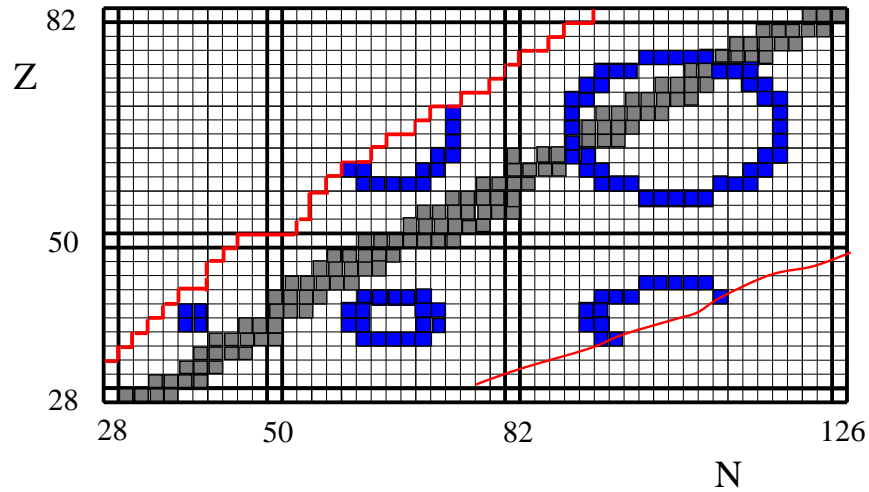


Figure 6.2. Nuclear regions with possible X(5) candidate nuclei (having $P \approx 5.0$) (courtesy of N.V. Zamfir).

A convenient indicator related to the spherical-deformed phase transitions is the quantity $P = N_n N_p / (N_n + N_p)$ – with $N_n(N_p)$ the number of valence neutrons (protons), which can be used to locate new candidates for the X(5) symmetry, since P passes through a value of 5.0 in the vicinity of the first order phase transition. As seen in Fig. 6.2, this occurs only for two regions near stability, including the above mentioned $N = 90$ isotones. It will be possible with AGATA to test this prediction also for the very exotic nuclei, like the very neutron-rich Mo or Ba isotopes. This could also give clues on the robustness of the next closed shells.

Another shape phase transition which can be studied with AGATA is the prolate-oblate transition that is expected below the $Z=82$, $N=126$ shell closures. Here the phase transition becomes even a triple point of nuclear shapes as all three phases touch each other (Figure 6.3).

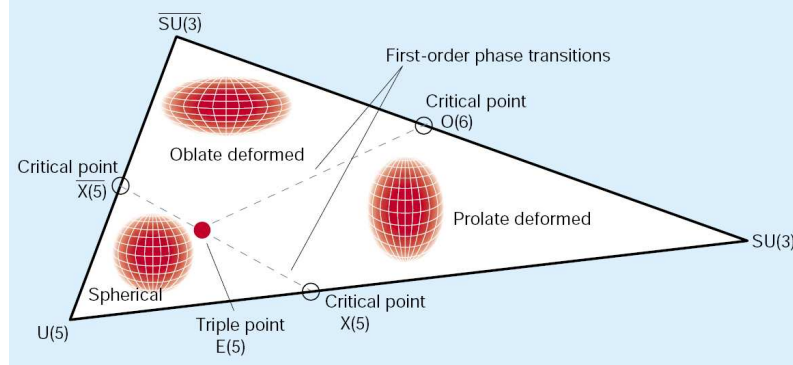


Figure 6.3. Schematic representation of the simplest shape phase diagram [6.6].

References

- [6.1] J. Jolie et al., Phys. Rev. Lett. 89(2002)182502.
- [6.2] D. Tonev *et al.* Phys. Rev C69(2004)034334.
- [6.3] F. Iachello, Phys. Rev. Lett. 87(2001)052502.
- [6.4] F. Iachello, Phys. Rev. Lett. 85(2000)3580.
- [6.5] R.F. Casten and E.A. McCutchan, J. Phys. G34(2007)R285.
- [6.6] D.D. Warner, Nature 420(2002)614.

7 Exploring the limits of nuclear rotation: Extreme nuclear deformations

The study of rapidly rotating, highly excited nuclei has been one of the main topics of the nuclear structure research over the last decades, and has been most rewarding in revealing a wide spectrum of nuclear structure phenomena which provide unique information on the detailed structure of the nuclear potential. The response of the nucleus to large amounts of angular momentum manifests itself in a range of phenomena involving shape changes and various types of rotational damping at higher excitation energy relative to yrast.

7.1 Superdeformation and hyperdeformation

One of the most striking shape changes is the superdeformation (SD). The study of very elongated nuclear shapes and their stabilization (due to shell effects) at high angular momentum has allowed the mean field description to be extended from normal to extreme deformation, putting its predictions under very severe tests. Nowadays we know some 200 SD bands, but, in spite of much experimental effort, for most of them the excitation energy, spin and parity, lifetimes, as well as their decay and feeding pattern are not known. This situation gives a good measure of the capabilities of the existing gamma arrays. The characteristics of a new generation array like AGATA will allow addressing all these questions. A special situation is met in the light nuclei, where the observation of SD bands is a domain opened only recently. In such nuclei (e.g., ^{36}Ar), the observed SD band is fully characterized: the energies and spins are known and the band was observed up to the maximum spin of the band configuration (the terminating 16^+ state) [7.1]. In addition,

in such light nuclei one can perform full, large scale shell model calculations, which offer a microscopic understanding of the phenomenon. Such "complete" observations in heavier nuclei would be extremely valuable, and a comparison between microscopic and mean field calculations very challenging. In isolated cases, the determination of the SD bands in heavier nuclei (mass ~ 130) has been made up to the band termination, or even beyond that. Such detailed studies allow the evolution of collectivity and shape with spin to be followed, thus providing information on the important nucleon orbitals involved.

Hyperdeformed (HD) structures, with frequency ratios along the short- and long axes of around 3:1, have been predicted theoretically for a long time in various mass regions. Experimental evidence exists in actinide nuclei from fission transmission resonance experiments. Here the extremely elongated shapes are stabilized by the Coulomb force. In lighter nuclei, the HD structures are predicted at very high spins where centrifugal and Coriolis forces play an important role. Shell corrections to the liquid-drop energies are not as large as those for superdeformation. However, if the macroscopic energy surfaces are sufficiently flat as a function of deformation in order to enable the shell effects and hyperintruder orbitals to produce sufficiently deep minima, HD structures may come sufficiently close to yrast to be populated in nuclear reactions. This condition is expected to be fulfilled at the highest angular momentum close to the fission limit where the Jacobi shape transition is expected to dominate.

Large energy gaps in the proton and neutron Routhian spectra appear at $Z = 48 - 54$ and $N = 70 - 73$ at a beta value of around 0.9. These gaps are crossed by hyper-intruder orbitals, like the $N=7$ proton orbital in the $N=4$ shell and the $N=8$ neutron orbital in the $N=5$ shell, with very strong deformation driving effects.

The search for discrete-line HD rotational bands with very large moments of inertia in various experiments, including a recent very long-lasting fusion-evaporation measurement producing the compound nucleus ^{128}Ba , did not reveal statistically significant candidates. However, the analysis of quasi-continuum gamma-ray correlation spectra has shown ridges presumably formed by cascading transitions corresponding to HD bands, for which the energy increases regularly with spin (Ref. [7.2]). An instrument like AGATA with its highly increased efficiency and resolving power is likely to open an exciting new era of gamma-ray spectroscopy in the HD well.

The limits in angular momentum can be pushed further with fusion reactions induced by neutron-rich projectiles, which populate larger angular momentum values than the stable beams, due to an increased value of the fission barrier with increased neutron number.

7.2 Jacobi shape transition

At very high spins, another spectacular shape change is expected to occur, which is related to the "Jacobi shape transition". At a certain critical angular momentum, a nucleus idealized as a charged incompressible liquid drop with surface tension, changes its equilibrium shape from an oblate spheroid to a triaxial ellipsoid, more and more elongated, rotating about its shortest axis (analogue phenomena are expected to take place in rotating stars). For example the predicted shape evolution for ^{46}Ti , obtained within the newest version of the liquid drop model LSD, is shown in Fig.7.2.1a. As angular momentum increases, the nucleus originally spherical at $I=0$ acquires some oblate deformation, corresponding to an elongation of up to $\beta=0.3$ for $I=26\hbar$. Beyond spin $26\hbar$, the Jacobi shape transition is predicted indeed: the nucleus becomes triaxial with the elongation parameter increasing up to values of $\beta > 1$ for $38\hbar$, and the fission finally takes place around $I=40\hbar$. Unlike

the SD shapes, the elongation occurs due to the centrifugal forces, at very high spins, and over a wide range of nuclei. Experimental indications of Jacobi shape phase transition have been obtained so far through the study of the giant dipole resonance (GDR) for the light hot nuclei around $A=46$. Namely, for ^{46}Ti the experimental GDR line shape at highest angular momenta was found to be characteristically split forming a narrow low-energy component around 10 MeV, and a broad structure ranging from 15 to 27 MeV (Fig. 7.2.1b). This line shape is consistent with the simulation of the GDR line shape for the Jacobi regime (Fig. 7.2.1c), based on the LSD results and thermal shape fluctuation model. This large splitting is a consequence of both the elongated shape of the nucleus undergoing the Jacobi shape transition and strong Coriolis effects which additionally split the low energy component (at about 13 MeV) by the value of $2\omega \approx 6$ MeV (where ω is the rotational frequency) and shift a part of its strength down to 10 MeV. For the oblate

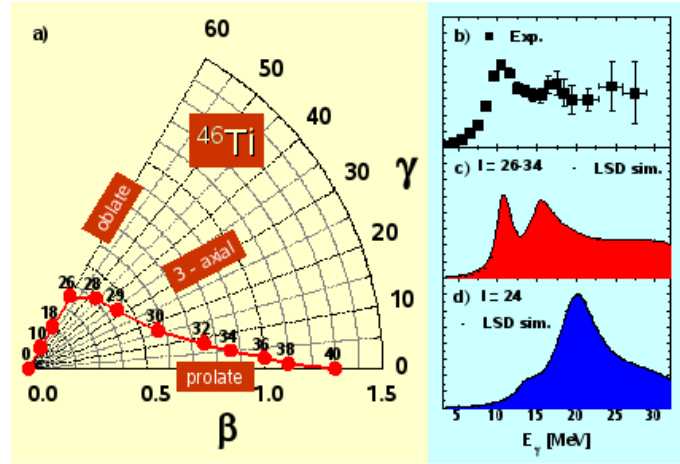


Figure 7.2.1. a) Spin evolution of the equilibrium shape of ^{46}Ti from the LSD model; b) Experimental GDR line shape for ^{46}Ti at high angular momentum; c) Predictions of the GDR line shape for spin region $26-34\hbar$, simulated with the LSD model; d) Same as c), but for $I=24\hbar$ (courtesy of A. Maj; see also Refs. [7.3]).

regime at $24\hbar$ (Fig. 7.2.1d), the calculated GDR line shape has the usual form of a broad Lorentzian distribution. Additionally it was suggested, that the low energy component of the Coriolis split GDR in the hot compound ^{46}Ti nucleus feeds preferentially the highly-deformed band in the cold ^{42}Ca evaporation residue. This might indicate that the Jacobi shape transition mechanism constitutes a gateway to the production of very elongated (hyperdeformed), rapidly rotating and relatively cold nuclei. Extension of such studies to medium mass and heavy systems, especially neutron-rich where the spin-window for Jacobi regime is generally wider, is of considerable interest.

For cold nuclei, the signature of a Jacobi shape transition is a sharp giant backbending in the plot of the energy of the bump of quasi-continuous quadrupole γ -ray transitions from the rotational states as a function of the angular momentum. With very efficient (both for low and high gamma energies) detector systems one will be able to study the possible correlations between the low energy component of the GDR and the quasi-continuous quadrupole 'bump'.

7.3 Shapes with broken axial symmetry

Theory has predicted nuclei with stable triaxial shapes for a long time. However, experimental proof for deviations from axial symmetry was, until recently, elusive. Although many observations could be explained in terms of triaxiality, these explanations were not unique. A triaxial nucleus may rotate collectively about any axis, and a unique effect of triaxiality is related to the extra degree of freedom by transferring some collective angular momentum from the axis with the largest moment of inertia to the two other axes. This transferred angular momentum is quantized, and a family of rotational bands with increasing number of wobbling phonon excitations is expected, with a characteristic decay pattern of competing inter-band and in-band E2 transitions. Wobbling has been identified in a number of even-N Lu-isotopes, including even a second phonon wobbling excitation in a couple of cases. The degree of freedom exploited in the wobbling excitation mode, studied in details with AGATA, will offer a unique possibility for determining three different moments of inertia for the rotational motion of a triaxial nucleus, a new challenge to theory. Likewise, the case of anharmonicity in higher (2nd) phonon wobbling excitations may be studied.

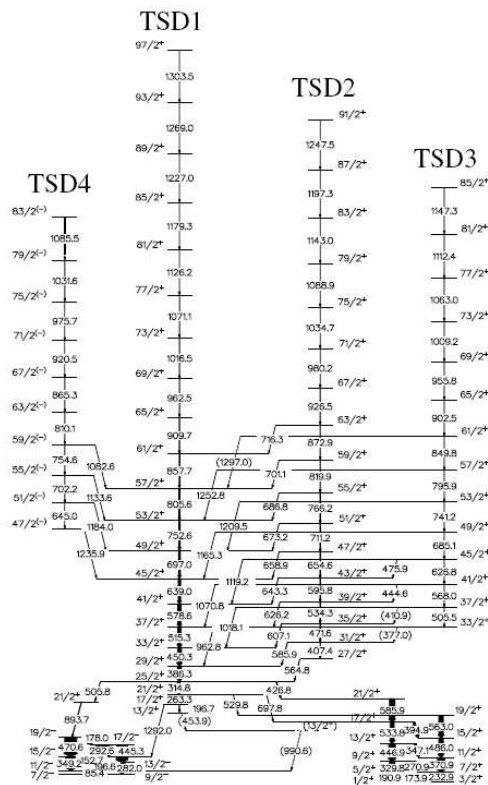


Figure 7.3.1. Wobbling bands in the triaxial nucleus ^{163}Lu [7.4].

The recently discovered 'nuclear wobbling' in odd-A Lu isotopes (Fig. 7.3.1) is such a mode which is a unique fingerprint of stable triaxiality. Families of rotational bands were observed which are built on the same intrinsic structure but with a fraction of the collective angular momentum transferred from the axis of largest moment of inertia to the two other axes of the triaxial nucleus. A characteristic decay pattern of competing inter-

band and in-band transitions was proof of wobbling excitations. However, it is strange and disturbing for the whole concept that wobbling was only observed in the odd-A Lu isotopes and not in their odd-odd neighbors and in other nuclei in this mass region where bands with similar moments of inertia were found. Do the wobbling excitations occur in those nuclei at higher energies and are they populated with less intensity, so that they could, therefore, not be detected with present-day spectrometers? AGATA will answer these important nuclear-structure questions.

Nuclear chirality or handedness in triaxial nuclei is characterized by three angular-momentum vectors, which have to be non-coplanar. In the case of an odd-odd nucleus the three vectors are composed by the valence proton, the valence neutron and the collective rotation of the core. The observation of two almost degenerate $\Delta I = 1$ rotational bands with the same parity in odd-odd nuclei (mainly) has so far been taken as a signature of the chiral geometry. Several examples of such bands have been found but none of the cases observed presents all the decay characteristics predicted theoretically, so that further cases and more detailed measurements are needed. One should emphasize that the information needed in order to understand the triaxiality of deformed nuclei is found in *experimental details*. For unambiguous interpretation, one needs precise energy and angle determination of the gamma rays, it is important to assign multipolarities and measure mixing ratios, pick up and correctly assign weak transitions, and for this one needs strong instruments like AGATA.

Until now, an impressive amount of good quality data highlighted various exotic shape phenomena, as emphasized above, but new phenomena are predicted and wait for experimental confirmation. As an example, various realistic mean-field calculations of nuclei with non-spherical symmetry predict the possible existence of exotic nuclei having *tetrahedral symmetry* possibly even in the ground state. The so far hypothetical presence of tetrahedral symmetry in nuclei is a result of advanced microscopic calculations based on the nuclear mean-field theory [7.5], which also predicts the well known magic numbers as a consequence of the spherical symmetry. In analogy, the tetrahedral symmetry leads to its own set of magic numbers: $Z, N = 32, 40, 56, 64, 70, 90, 106$, and ($N=132$). Consequently, combinations of the proton and neutron numbers from the vicinity of the magic ones are predicted to result in the presence of several islands of nuclei with the shape coexisting minima of tetrahedral symmetry.

In some nuclei such as ^{96}Zr or the very exotic ^{110}Zr , calculations suggest that the ground state shapes are of tetrahedral symmetry. A more detailed analysis indicates that such nuclei will combine the excitation properties characteristic of spherical nuclei (i.e. in accordance with the experimental results known today for ^{96}Zr) with extra features related to the tetrahedral symmetry. Among most important predicted properties of nuclei with tetrahedral symmetry is the vanishing quadrupole moments. Consequently, in the tetrahedral nuclei rotational bands should exist, however the E2 transitions are expected to vanish or be very weak. Fig. 7.3.2 shows the total energy surface for a doubly magic tetrahedral nucleus: ^{154}Gd ($Z=64, N=90$). In fact, in its neighbor ^{156}Gd , a band with the characteristic predicted properties has already been seen (Fig. 7.3.3). The quadrupole transitions for $I^\pi \leq 9^-$ have never been seen experimentally although more than a dozen of various experimental setups and reactions have been used to try to establish the corresponding decay. Nuclei with similar properties exist in several islands throughout the periodic table, and are predicted for many exotic and very exotic nuclei. The experimental approach of such nuclei requires the use of the new generation of γ -ray detectors.

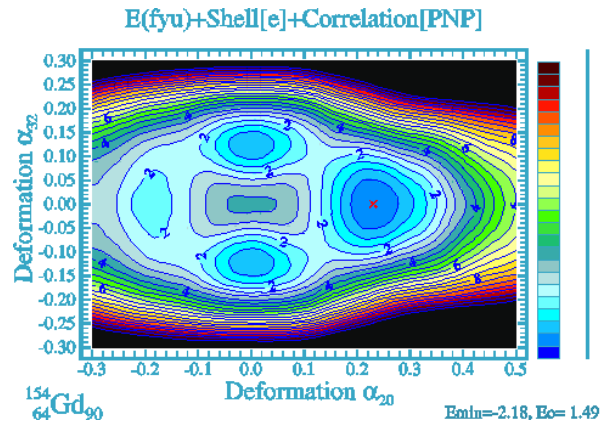


Figure 7.3.2. Total energy surface calculated using a realistic mean-field approach. Observe the presence of the prolate ground-state, the oblate competing minimum for the negative quadrupole deformation α_{20} and the two low-lying symmetric minima at the deformation α_{32} which models the tetrahedral symmetry.

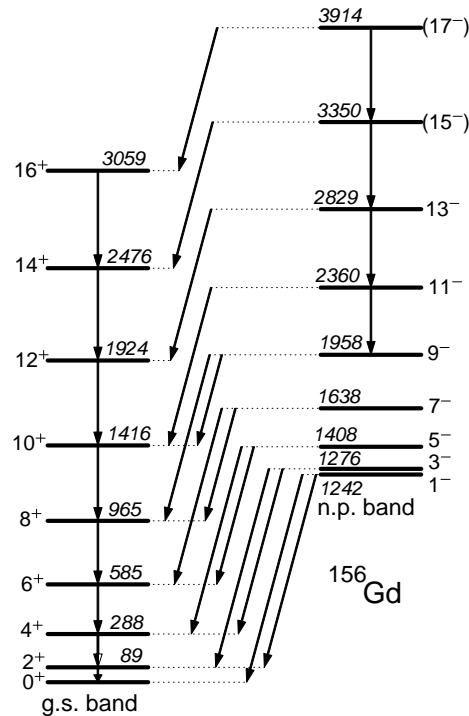


Figure 7.3.3. Experimental partial decay scheme of ^{156}Gd .

7.4 Magnetic rotation

Traditionally it was understood that rotational bands can only occur in nuclei with a deformed charge distribution, while spherical or near-spherical nuclei show spectra of single-particle excitations. The observation of rotational-like sequences of strongly enhanced magnetic dipole transitions in several light-mass Pb isotopes was, therefore, very surprising. These isotopes were known to have very small deformations and, yet, the

bands showed a remarkable regularity, like the ones that were so far only observed in well deformed nuclei.

It is now understood that this type of rotational bands can occur when the symmetry of the quantal system is broken by anisotropic currents connected with certain high-spin particle and hole excitations. With the anisotropic currents large magnetic moments rotate about the direction of the total angular momentum. Therefore, this type of excitation was named *magnetic rotation* to distinguish it from the long-known rotation of deformed nuclei.

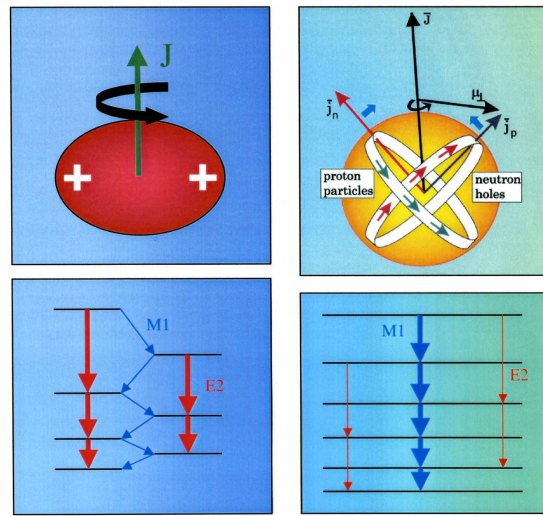


Figure 7.4.1. Pictorial representation of deformed nucleus rotation bands and nuclear magnetic rotation bands.

The cleanest cases of magnetic rotation occur in neutron-deficient Pb isotopes [7.6]. Examples observed in other mass regions also exist. However, it is rather conspicuous that such bands have not been found in other nuclei close to the Pb isotopes, e.g. in Bi or Po nuclei where the deformation is equally small and the same particle and hole excitations are low in energy. This poses a severe question for the physical picture of magnetic rotation which needs to be answered by AGATA.

Another important open question is that of the behavior of the crossover E2 transitions as a function of spin within the magnetic-rotational bands. Since the transition probabilities depend on the angle of the axis of the small deformation with the angular momentum axis, they can decide between different theoretical approaches.

Due to the small deformation the E2 rates are small and the transitions are difficult to detect with present spectrometers. With AGATA, precise intensities of the E2 transitions will be measured, which will finally refine the underlying physical picture.

References

- [7.1] C.E. Svensson, Phys. Rev. Lett. 85(2000)2693.
- [7.2] B. Herskind *et al.*, Acta Phys. Pol. B34(2003)2467.
- [7.3] M. Brekiesz *et al.*, Nucl. Phys. A788(2007)224c; A. Maj *et al.*, *ibid.* A752(2005)264c.
- [7.4] D.R. Jensen *et al.*, Eur. Phys. J. A19(2004)173.
- [7.5] J. Dudek *et al.*, Phys. Rev. Lett. 88(2002)252502.
- [7.6] R.M. Clark *et al.*, Phys. Rev. Lett. 78(1997)1868.

8 Highly excited states and nuclei at finite temperature

8.1 Order-to-chaos transition

The investigation of the rotational motion as a function of temperature plays a crucial role in the understanding of the properties of the nuclear system beyond the mean field description, providing relevant information on the two-body residual interaction responsible for the band mixing process. Close to the ground state, the low-lying excited states are characterized by good intrinsic quantum numbers and consequently their decays are governed by selection rules. At higher energies, the level density and level mixing increase very much, therefore the concept of quantum numbers is broken; the disappearance of the quantum numbers (and of the associated symmetries) is a signature of quantum chaos. Experimental evidence is found that at 6-8 MeV of thermal energy (neutron separation energy) the neutron resonances are well described by the random matrix theory, therefore in the "warm" region, lying in between the regular ground state regime and the chaotic region, there must be a transition from order to chaos. This is the region where the *rotational motion is damped*, due to the rapid increase in the level density and to the presence of a residual interaction which mixes the close lying states. As a consequence, the rotational E2 γ -decays from the compound states at spin I becomes fragmented over many final states at spin I-2. The width of this strength function is the so-called rotational damping width Γ_{rot} , its magnitude being directly related to the evolution of the nuclear system towards complexity. Consequently, the study of the rotational damping regime is crucial for the understanding of where and how the chaotic behavior sets in [8.1, 8.2, 8.3].

Experimental efforts in studying the order-to-chaos transition mostly concentrate on the investigation of rotational damping as function of mass, deformation, and intrinsic configuration. This will strongly benefit from the selectivity of the high-fold γ -ray coincidence data of AGATA. In fact, by selecting particular decay paths the dependence of the damping width on spin and excitation energy will be tested, allowing to observe exotic effects associated with chaos, such as motional narrowing and ergodic bands [8.4]. While the first is predicted to occur at rather high excitation energy (≥ 2 MeV above the ground state), the second one (a non-fragmented rotational decay between practically chaotic states) is expected to be observed more likely in heavy nuclei and/or highly deformed shapes. The strong variation of the rotational damping width with neutron/proton number, as predicted by microscopic cranked shell model calculations at finite temperature [8.5], will also be studied with AGATA, giving information on shell structure effects beyond mean field. As shown in Fig. 8.1.1, in the case of Yb isotopes, an increase of the damping width of $\approx 25\%$ is predicted in going from ^{168}Yb to ^{176}Yb , almost entirely due to neutron shell effects.

8.2 Giant resonances

The nuclear giant resonances (GR) are collective states at high excitation energies (with most strength above the particle separation threshold) which represent a coherent motion involving many nucleons. Their features are therefore governed by macroscopic nuclear properties such as size (radius), shape, (neutron) skin, compressibility, viscosity, etc. Microscopically, they are understood as coherent 1p-1h excitations that are determined by the effective nucleon-nucleon interaction. Many such modes are known, as studied with different probes of various selectivity, and are classified according to their quantum numbers, such as multipolarity, spin, and isospin.

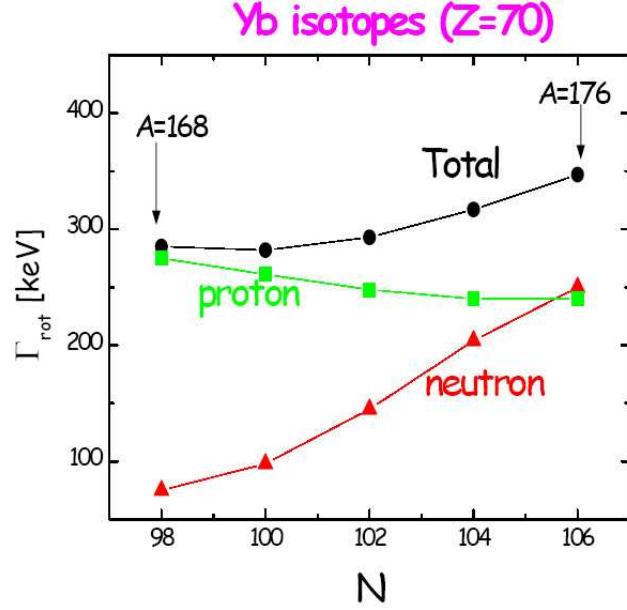


Figure 8.1.1. Shell effects on rotational damping: in Yb isotopes the rotational damping width Γ_{rot} (circles) increases $\sim 25\%$ from $A=168$ to $A=176$, mostly due to neutron shell effects. The calculations are performed at spin $I=40\hbar$ and thermal energy $U \approx 2$ MeV [8.5].

The study of the γ -decay from nuclear resonance states will strongly benefit from the high efficiency and good energy resolution of the AGATA array, which will provide not only systematic data on giant resonance states at zero temperature, such as Giant Quadrupole (GQR) and Giant Dipole (pygmy) collective modes, but it will also allow to investigate in detail resonance states built on excited states. Since the dipole resonance couples to the nuclear deformation the investigation of its strength function provides information on the nuclear shapes. Of particular interest is the search of superdeformed and Jacobi shapes at finite temperature.

At zero temperature, the study of the GQR (a collective vibration where both the shape and the nucleon distribution change) will provide direct information about the effective N-N interaction, from which the E2 response of the system strongly depends. The excitation of giant resonances with inelastic scattering of heavy ions at few tens of MeV/u does not have an angular distribution characteristic of the multipolarity of the mode, but it can still be used for the decay studies because of its enhanced cross section in comparison with light ions. In fact, particle and gamma decay from giant resonances probe in detail the microscopic structure of giant resonances and its damping mechanisms. In addition, from the investigation of the γ -decay channel the multipolarity of the excitation can be inferred [8.6].

In the case of the dipole resonance (GDR) one of the main questions is the evolution of the giant dipole resonance strength with the neutron to proton number ratio (from stable to exotic/weakly bound nuclei). Nowadays, the general feature of the existing calculations is the redistribution of the strength towards lower excitation energies (well below the giant resonance region), and the details of these redistribution are found to strongly depend on the effective forces used in the model. The low-energy part of the GDR strength func-

tion (often referred to as pygmy resonance) is proposed to arise from the vibration of the less tightly bound valence neutrons against the residual core. Consequently, the measurements of the GDR strength function in unstable nuclei is expected to provide important information on the isospin dependent part of the effective nucleon-nucleon interaction and on dipole type vibrations of excess neutrons. Experimentally, the pygmy resonance can be studied by Coulomb excitation reactions, therefore such kind of measurements will strongly benefit from the use of the AGATA, particularly when using inelastic scattering at high bombarding energy.

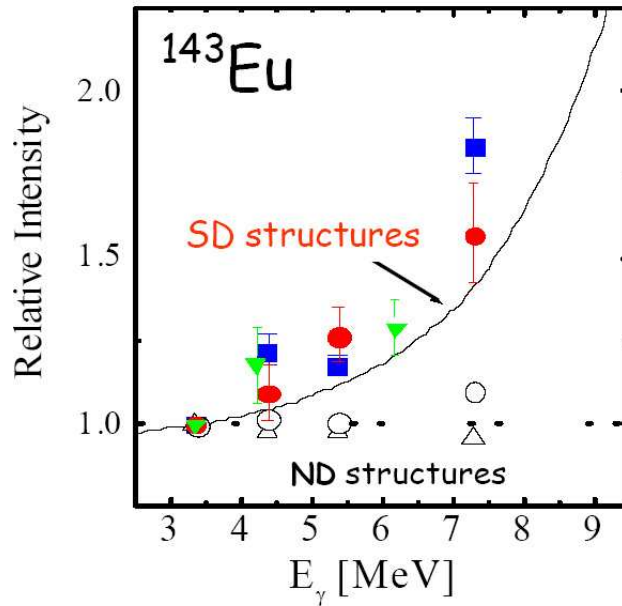


Figure 8.2.1. The relative intensity of the superdeformed (SD) structures in ^{143}Eu (filled symbols) is found to increase when a coincidence with high-energy γ -rays from the GDR resonance is requested. This is not observed in the case of the normal deformed (ND) structures (open symbols) – adapted from Ref. [8.7].

High-fold γ -ray coincidence data with the selectivity of AGATA will also be crucial for the investigation of vibrational collective modes at finite temperature. This is, for example, the case of the preferential feeding of the highly deformed structures in residual nuclei by the GDR low energy component, as found in the superdeformed ^{143}Eu nucleus (cf. Fig. 8.2.1). This is an interesting open problem which requires new investigations in other nuclei and with the sensitivity and efficiency of AGATA one expects to provide relevant results on this topic. Another example is the study of the Jacobi shape transition (a nuclear shape change at high angular momenta from oblate to triaxial and very elongated prolate) [8.8] which can be inferred from the splitting of the GDR strength function towards lower energy, at the most extreme values of angular momenta.

Finally, another interesting problem is the high-energy gamma emission in the formation process of the compound nucleus in fusion reactions. This pre-equilibrium emission gives information on the charge equilibration time and depends on the symmetry energy at low nuclear density. In particular, reactions with very different values of the N/Z of the target and projectile are characterized by the presence of the so-called dynamical mode,

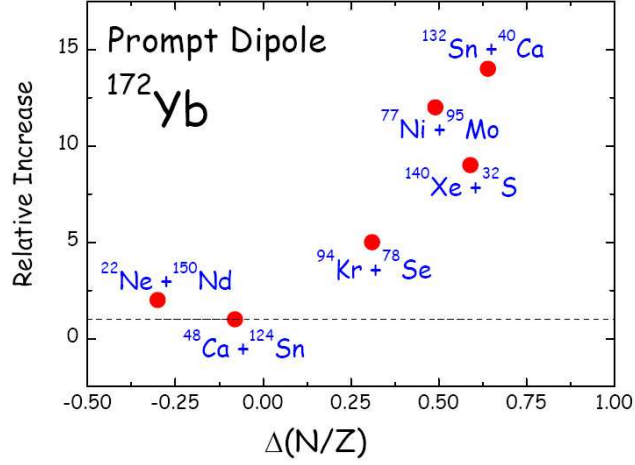


Figure 8.2.2. The yield of the GDR emission in pre-equilibrium fusion reactions leading to the compound nucleus ^{172}Yb is expected to increase significantly with the N/Z asymmetry of the projectile-target system. The points are calculated according to the model of Ref. [8.9].

which consists in pre-equilibrium dipole radiation emitted by a fusing system [8.9,8.10]. This emission is characterised by a low energy centroid, 10 MeV, and can be isolated from the contribution of the GDR emitted after the equilibration of the system by comparing the E1 yield of two different reactions leading to the same compound nucleus, at the same excitation energy and spin: one (symmetric) employing target and projectile with similar N/Z and one (asymmetric) with projectile and target with very different N/Z. As shown in Fig. 8.2.2, the yield of this prompt dipole radiation is expected to increase by more than an order of magnitude making use of more and more N/Z asymmetric systems.

8.3 Level densities and gamma-ray strength functions

The structure of unresolved states in continuum can be investigated with statistical methods. The Oslo group has developed a method that reveals simultaneously the density of levels and the gamma-ray strength functions from these levels [8.11]. The experiments are performed with light-particle inelastic or transfer reactions in coincidence with gamma rays. The charged ejectile is used to tag excitation energies for each gamma-ray spectrum from the ground state up to the neutron (or proton) binding energy.

These types of experiments have given evidence for the transition from a superconducting to a normal Fermi gas phase as function of temperature. In the rare earth region, the pairing correlations are quenched at a critical temperature of $T_c \approx 0.5$ MeV. Furthermore, the tail of the GEDR for gamma energies between 1 and 8 MeV has been investigated.

Figure 8.3.1 shows the entropies for $^{160,161}\text{Dy}$ extracted from the level density as $S = \ln(\rho/\rho_0)$ [8.12]. This is the starting point to deduce other thermodynamic quantities as temperature T and heat capacity C. In Fig. 8.3.2 is illustrated how the method reveals the M1 scissors mode in continuum.

A very interesting idea is to extend the Oslo method to inverse kinematics. There are several topics that can be studied with the combination of AGATA and rare ion beams. In particular, far from the beta-stability line, very limited information exists on nuclear level density, thermodynamic properties, gamma-ray strength functions and pygmy resonances.

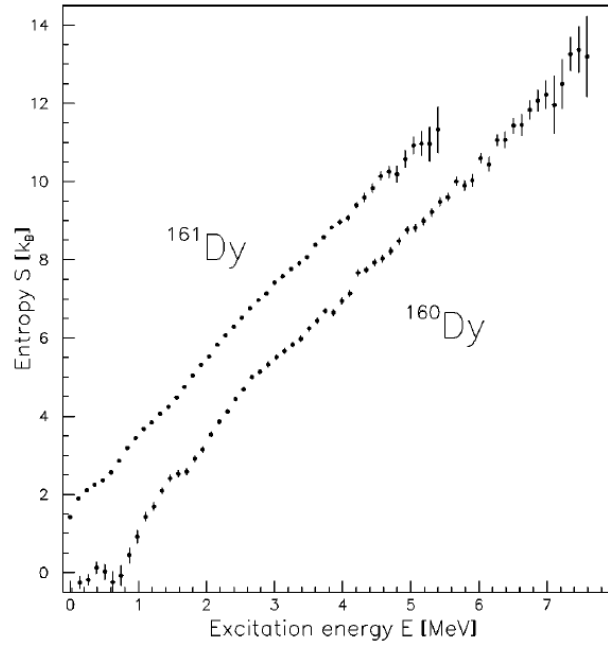


Figure 8.3.1. Entropy as a function of the excitation energy for $^{160,161}\text{Dy}$.

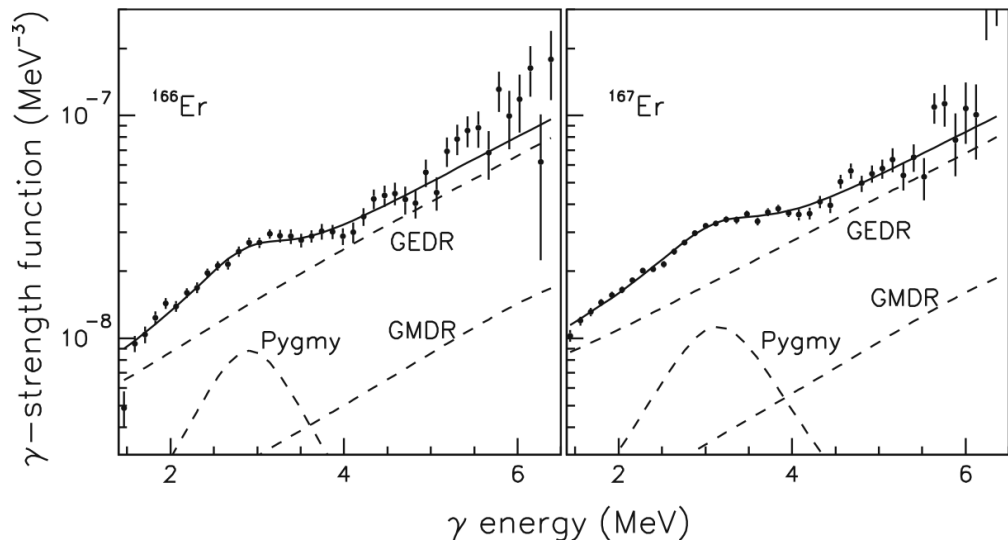


Figure 8.3.2. Gamma-strength functions for $^{166,167}\text{Er}$.

References

- [8.1] A. Bracco and S. Leoni, Rep. Prog. Phys. 65(2002) 299.
- [8.2] M. Matsuo *et al.*, Nucl. Phys. A617(1997)1.
- [8.3] S. Leoni *et al.*, Phys. Rev. C72(2005)034307.
- [8.4] B. Mottelson *et al.*, Nucl. Phys. A557(1992)717c.
- [8.5] M. Matsuo *et al.*, Nucl. Phys. A649 (1999)379c.

- [8.6] J. Beene *et al.*, Phys. Rev. C39(1989)39.
- [8.7] G. Benzoni *et al.*, Phys. Lett. B540(2002)199.
- [8.8] W.D. Myers and W.J. Swiatecki, Acta. Phys. Pol. B32(2001)1033.
- [8.9] C. Simenel *et al.*, (Phys. Rev. Lett. 86(2001)2971).
- [8.10] V. Baran *et al.*, Phys. Rev. Lett. 87(2001)182501.
- [8.11] A.Schiller *et al.*, Nucl. Instr. Meth. Phys. Res. A447(2000)498.
- [8.12] M.Guttormsen *et al.*, Phys. Rev. C68(2003)064306.

9 Structure of superheavy nuclei

A long standing question in nuclear physics is *where is the limit of existence of the heaviest nuclei?* This is related to the understanding of *the balance between the strong force and the Coulomb interaction in superheavy nuclei which allows a bound nuclear system?*

Apart from synthesizing superheavy isotopes, it is important to study their structure in order to understand the physics in a complete and coherent way, and to acquire detailed data which can be used to refine state-of-the-art nuclear structure theories. By studying high-spin states, K-isomers, and rotational bands in superheavy nuclei it is possible to pin down the positions of the single-particle levels, determine the deformation and hence gain access to shell properties of these nuclei. The production cross sections of transfermium nuclides are sufficiently high to make it possible to carry out detailed spectroscopic studies. Already with the present arrays spectroscopic studies on transfermium nuclides have been carried out (see Fig. 9.1), but the AGATA spectrometer will further enhance this research, allowing detailed studies of nuclei with higher proton number to be studied.

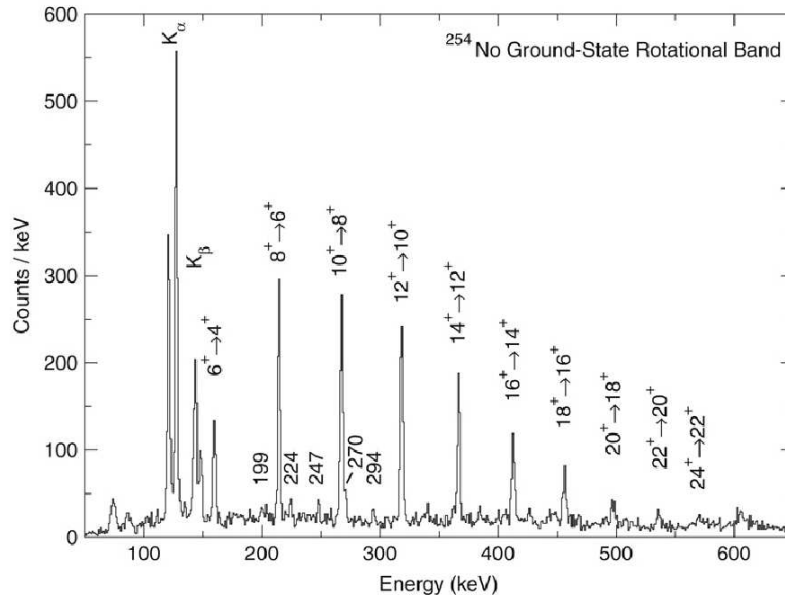


Figure 9.1. Recoil-gated gamma-ray spectrum of ^{254}No obtained in experiments using RITU, GREAT and JUROGAM. (Refs. [9.1, 9.2]).

Some of the objectives for near future are:

- to determine the orbits responsible for the configuration for such nuclei;

- to study the collectivity of the nuclei, and in particular the "island of deformation" around ^{254}No and ^{270}Hs ;
- to study the role of K-isomerism.

This research requires very intense stable beams and a spectrometer with very high acceptance and good beam rejection, in combination with a gamma-spectrometer with very high resolution and very high granularity, able to handle very high counting rates (AGATA). Since these nuclei have very high proton number, internal conversion dominates in the decay of the low-energy transitions. It is therefore of interest to consider the coupling of AGATA to an electron spectrometer for simultaneous electron-gamma coincidence measurements. Such a device (SAGE) is currently being developed by the University of Liverpool and Daresbury Laboratory to be hosted at JYFL and coupled to JUROGAM and RITU.

References

- [9.1] R.-D. Herzberg *et al.*, Nature 442(2006)896.
- [9.2] R.-D. Herzberg and P.T. Greenlees, Progr. Part. Nucl. Phys. 61(2008)674.

Appendix 1: Hypernuclei

A hypernucleus contains one or more hyperons implanted into a nucleus. In this way, one adds a third dimension - the strangeness quantum number - to the nuclear chart, extending our knowledge of matter. The hyperon may be used as a probe for the nuclear structure, and its possible modifications due to its presence. On the other hand, it is interesting to see how the properties of the hyperon itself modify when it is implanted inside a nucleus. Measurements of level schemes and decay properties of such strange exotic objects as hypernuclei, allow microscopic structure models based on various baryon-baryon interactions to be tested. Today, about 35 $S=-1$ hypernuclei (Λ - and Σ -hypernuclei) and four $S=-2$ hypernuclei ($\Lambda\Lambda$, Ξ) have been observed, in the light mass region. The spectroscopy of multi-strange hypernuclei - the hypernuclear gamma spectroscopy, provides information on the baryon-baryon interaction; thus one can achieve a unified understanding of the baryon-baryon interaction from the ΛN interaction (meson and quark models) and the phenomenological NN interactions, through the nuclear structure. There are also so-called impurity effects, like change of size (shrinkage) and shape, new symmetries, and change of the collective effects.

At present, a drawback of the field, with impact to the development of the theoretical investigations, is the lack of high resolution and systematic data on single and multi-strangeness hypernuclei. The energy resolution of hypernuclear studies was limited to typical values of about 1 MeV, and only recently started to take advantage of the use of high-efficiency Ge arrays spectroscopy.

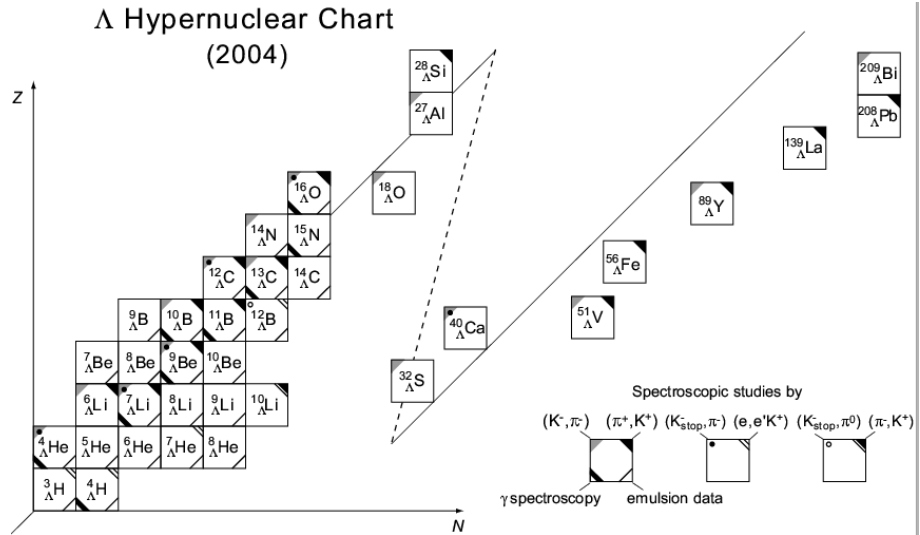


Figure A1. Chart of the known hypernuclei (courtesy of O. Hashimoto and H. Tamura).

The use of Ge detectors is absolutely necessary in order to observe the hypernuclear fine structure (the splitting of the nuclear levels due to the ΛN spin-dependent interaction), which may be as small as a few tens of keV. Detailed information, such as the observation of important gamma transitions in order to derive the Lambda-Sigma coupling force, and $B(E2)$ values to precisely determine the shrinking effect, require a gamma array of high performance.

Gamma-gamma coincidence studies have also been recently reported. In the best studied hypernuclei, like ${}_{\Lambda}\text{Li}^7$, ${}_{\Lambda}\text{Be}^9$, ${}_{\Lambda}\text{O}^{16}$, one could characterize the ΛN spin-spin, spin-orbit and tensor forces.

The hypernuclear spectroscopy will be a developing field, aiming at: a complete study of the light ($A < 30$) hypernuclei; systematic studies of medium and heavy hypernuclei; study of n-rich, p-rich, and pairs of mirror nuclei; measurements of spin-flip (M1) transition strengths; systematic investigation of double strangeness hypernuclei. Such systematic studies will have an important impact on our understanding of the nuclear forces and the nuclear medium effects of baryons. Such studies with AGATA at the anti-proton GSI ring, with appropriate solid state micro-tracker devices, will allow for the first time high-resolution gamma spectroscopy of double hypernuclei to be performed.

Appendix 2: Nuclear astrophysics

Understanding the nucleosynthesis processes which take place in the stellar environment is based on models that depend on many nuclear structure physics parameters, like nuclear masses, lifetimes, decay modes, level structures, level densities, reaction cross sections. As a rule, nuclear astrophysical data are very difficult to obtain, since many important nuclei are situated far from the line of stability and therefore are difficult to reach, and cross sections at the relevant energies are very small. The high efficiency and high rate possibilities offered by AGATA could be essential for crucial measurements in this field. Giant resonance studies (ch. 8.2) may be also relevant for nuclear astrophysics since many reaction rates at astrophysical conditions have giant resonance contributions.

Appendix 3: Fundamental interactions

Nuclear physics measurements constitute the most valuable tests of the fundamental symmetries underlying the Standard Model of the electroweak interactions. Such tests are provided by very precise measurements of the superallowed $0^+ \rightarrow 0^+$ Fermi beta transitions, or the Gamow-Teller transition rates in mirror nuclei, respectively. For example, the study of the superallowed $0^+ \rightarrow 0^+$ beta decay transitions allows first to test the *Conserved Vector Current (CVC) hypothesis*, whose consequence is the prediction that the measured ft values for all such transitions must be the same, regardless of the parent nucleus. This test was currently done for 13 nuclei (the heaviest ones being ${}^{62}\text{Ga}$ and ${}^{74}\text{Rb}$) and confirmed that the vector coupling "constant" G_V (or, the weak-interaction coupling constant) does not depend on the nucleus (is indeed a constant within one part in 10^4). This has allowed a determination of the V_{ud} element of the Cabibbo - Kobayashi - Maskawa (CKM) matrix, which is responsible for the mixing between the u and d quarks. With two other basic CKM matrix elements, V_{us} and V_{ub} , estimated from other sources, a test of the unitarity of the CKM matrix (which is required by the Standard Model) could be made. The unitarity was found to be well fulfilled, which sets important constraints on the physics beyond the Standard Model. The most important task now is to determine what new physics is possible within the existing uncertainty of the unitarity test. Thus, in deriving the CKM matrix elements both improvements in theory (the theoretical correction terms) and experiments are needed. New measurements on heavier $T_z = 0$ nuclei, which are expected to become available with the radioactive beams and new detecting equipment, will offer better tests of these crucial points of the Standard Model.

Appendix 4: AGATA technical characteristics and simulations

AGATA, the **A**dvanced **G**AMMA **T**racking **A**rray [A1-A4] is a 4π detector consisting of 180 HP germanium detectors. Each detector crystal is electrically segmented in 36 ways, giving a total of more than 6600 electronics channels. The detectors will be assembled into 60 triple cryostats. For each detector pulse a shape analysis will be performed in order to determine the interaction positions of the gamma radiation within the crystal to an accuracy of better than 2 mm. By using the energy and interaction position information, tracking algorithms will reconstruct the paths of the gamma rays through the detectors. The crystals have a length of 90 mm and hexaconical shape based on an 80 mm diameter cylinder. In the complete geometry the inner radius of the sphere will be 23.5 cm and the Ge detectors will cover 82% of 4π .

The energy resolution of individual detector segments is 0.9 to 1.1 keV at 60 keV, and 1.9 to 2.1 keV for 1.33 MeV gamma rays, respectively, and cross talk between segments is below 10^{-3} .

The first phase of the project is to build a system consisting of 5 triple cryostats containing 15 detectors, see Fig. A4.1. This is called the AGATA demonstrator and it is being commissioned at the Legnaro National Laboratories, starting in 2008.

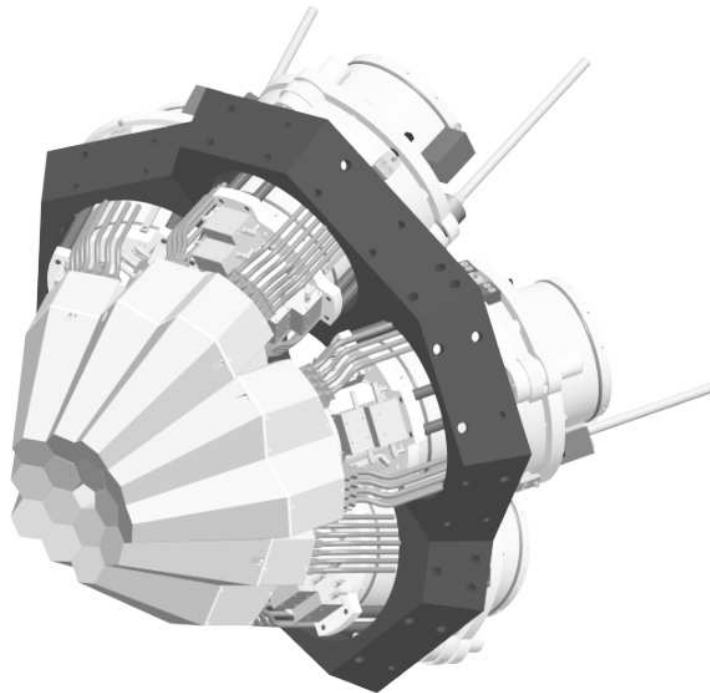


Figure A4.1. A computer design image of AGATA with 15 detectors (five triple modules) that will be operated in Legnaro starting in 2009.

The number of detectors in the array will be continually increased to the whole array with the expectation that it will be available around 2015. AGATA will be operated in a series of experimental campaigns at accelerator facilities in Europe. AGATA will be operated with many different ancillary detectors to study specific nuclear properties.

The expected performance of AGATA (estimated for a stationary pointlike source

placed in the centre, for 1.33 MeV gamma ray), has been simulated using a code based on Geant4 and developed by E. Farnea *et al.* [A5,A6]. The gamma-ray tracking was performed either by the MGT program developed by D. Bazzacco [A7] or by the program developed by A. Lopez-Martens *et al.* [8]. The predicted efficiency and peak to total for various multiplicities are given in the following table:

Multiplicity	1	10	20	30
Efficiency (%)	43.3	33.9	30.5	28.1
Peak to total ratio (%)	58.2	52.9	50.9	49.1

Such characteristics for the gamma-ray spectroscopy are unprecedented. *The high efficiency and P/T ratios* will allow studies of processes with low cross sections; for high-multiplicity, weakly populated gamma-ray cascades, as met in high-spin studies, the sensitivity will be several orders of magnitude higher than that of existing gamma-ray arrays, as illustrated in Fig. A4.2.

$^{28}\text{Si} + ^{28}\text{Si}@125\text{ MeV}$. Particle detection
with EUCLIDES. Kinematical recalibration.

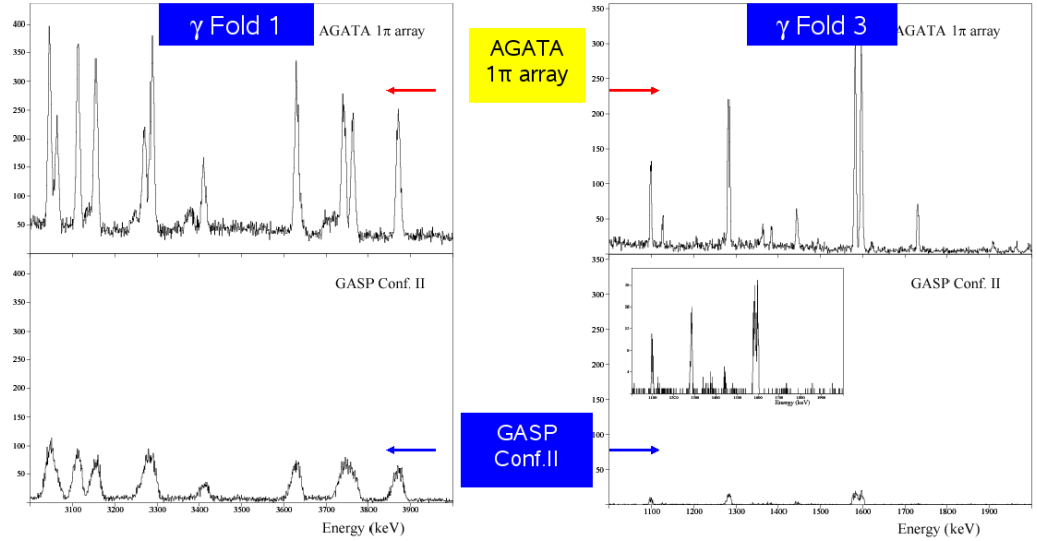


Figure A4.2. Comparison of the performances of 1π AGATA array with GASP [A9] in Configuration II (simulated experiment).

High efficiency and good energy resolution at high energies opens up completely new possibilities for studies of the giant resonances. The position resolution ensures an *angular resolution* much better than the segment size, therefore quite accurate Doppler corrections can be performed even in the case of relativistic recoiling products (velocities of tens of percents of c), as shown by the simulation in Fig. A4.3.

In addition, due to the segmentation and digital signal processing, the *counting rates will be up to 10 times higher* than the current ones, allowing higher beam currents and study of rare events. Due to the tracking, the array will have an increased sensitivity for gamma ray linear polarization measurements, which are essential for parity assignments, and, hopefully, it will give a high rejection of background events.

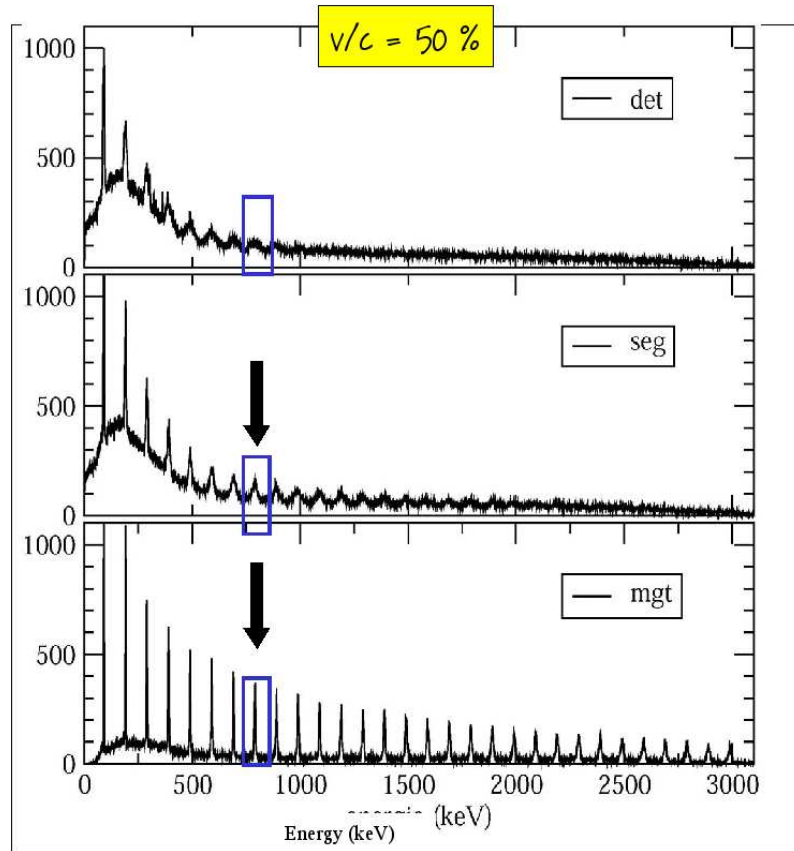


Figure A4.3. Effects of the Doppler correction for the AGATA array. Up: spectrum only from crystal information; middle: Doppler correction using only the segment information; bottom: Doppler correction performed with the tracking code *mgt* (simulation for a gamma-ray band with multiplicity 30).

The performance of AGATA will be enhanced by combining this array with appropriate *ancillary detectors*. Fig. A4.4 shows an example of the quality of the Doppler correction that could be obtained by coupling the AGATA demonstrator to the PRISMA [A10] spectrometer at Legnaro. The input events were ^{90}Zr ions uniformly emitted within a 10° cone around the entrance axis of the spectrometer, and having a Gaussian energy distribution around 350 MeV, with a FWHM of 35 MeV (a situation which simulates product nuclei from multi-fragmentation reactions). Each ^{90}Zr nucleus emits one 1 MeV gamma ray. The gamma-ray spectrum shown in Fig. A4.4 was constructed by using tracking within AGATA and recoil trajectory reconstruction in PRISMA. With the full information from PRISMA it is clearly possible to obtain effective energy resolution values very close to the intrinsic detector resolution, unlike the case when the CLARA array [A11] is used.

AGATA will make a major improvement in spectra quality and efficiency in a wide range of experimental conditions. Several simulations of different types of experiments have been performed. To illustrate AGATA's power, some examples of its performances will be shown, where the predicted performances of the AGATA demonstrator are compared with other spectrometers.

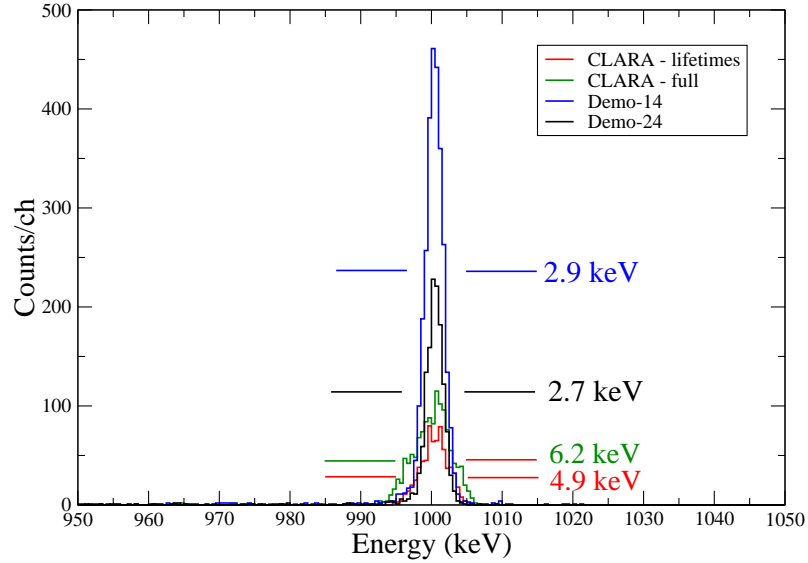


Figure A4.4. Comparison of Doppler-corrected gamma-ray spectra obtained with the AGATA demonstrator and the CLARA array, in coincidence with the PRISMA spectrometer. The simulated situation is: ^{90}Zr nuclei with a Gaussian energy distribution with 35 MeV FWHM, around 350 MeV, uniformly emitted over the PRISMA opening, and each one emitting one gamma-ray of 1 MeV. "Demo-14" and "Demo-24" refer to distances of 14 and 24 cm, respectively, from the target to the Ge shell.

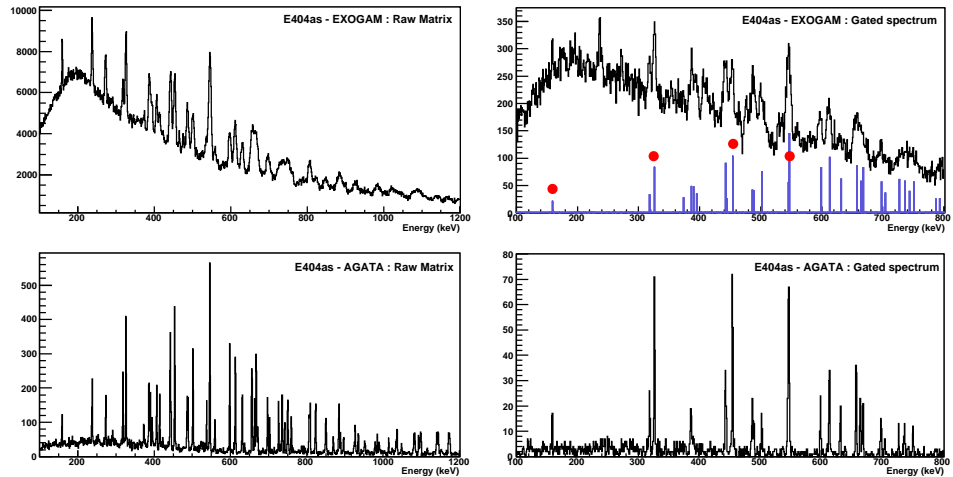


Figure A4.5. Comparison of simulated EXOGAM and AGATA demonstrator spectra. Left: total projection spectra. Right: spectra gated on the four most intense transitions of ^{130}Nd , marked by red points; the upper panel indicates also the expected transitions from the ^{130}Nd level scheme (courtesy of O. Stekowski).

The first example is that of a fusion evaporation reaction, where the AGATA demonstrator is compared with the EXOGAM spectrometer [A12]. The case considered is based on an experiment performed at GANIL with a 330 MeV ^{76}Kr radioactive beam from SPIRAL on a ^{58}Ni target, used to populate nuclei around the proton drip line. The mean

recoil velocity in this reaction is 4.7%.

Discrete gamma-ray cascades have been randomly generated (using the gammaware package, <http://agata.in2p3.fr>) from the level schemes of the six main residual nuclei (^{127}Pr , ^{129}Pr , ^{128}Nd , ^{131}Pm , ^{130}Pm , and ^{130}Nd) with relative cross sections as given by the EVAPOR code. Simulations [A5,A6] of both the AGATA demonstrator and EXOGAM were performed. The later consists of a configuration of 12 clovers (8 at 90° and 4 at 135°) at 11.4 cm from the target. A $\gamma-\gamma$ coincidence matrix was built for both simulations using, for AGATA, the tracking code of Lopez-Martens *et al.* [A8]. The simulated projection spectrum for the EXOGAM experiment compares reasonably well with the real data; the relative intensities of gamma-ray transitions are not perfectly estimated since the used level schemes were established in other experiments, but this does not affect the conclusions of the comparison.

The full projections of the two simulated matrices are displayed in the left panels of Fig. A4.5. The statistics of the EXOGAM spectrum is larger (because of the larger efficiency) but, despite a lower statistics, the spectrum obtained for the AGATA demonstrator contains much more information. It allows to disentangle the expected transitions over the complete energy range while for EXOGAM the opening angle of the clovers restricts precise measurements only to low energies (below 600 keV). The spectra in the right panels were obtained by gating on four of the most intense transitions belonging to the ^{130}Nd level scheme (marked with red points in the picture). The superiority of the AGATA spectrum is clearly displayed. The conclusion is that for medium spin spectroscopy with fusion-evaporation reactions, AGATA is an extremely powerful tool compared with EXOGAM, even in its demonstrator configuration.

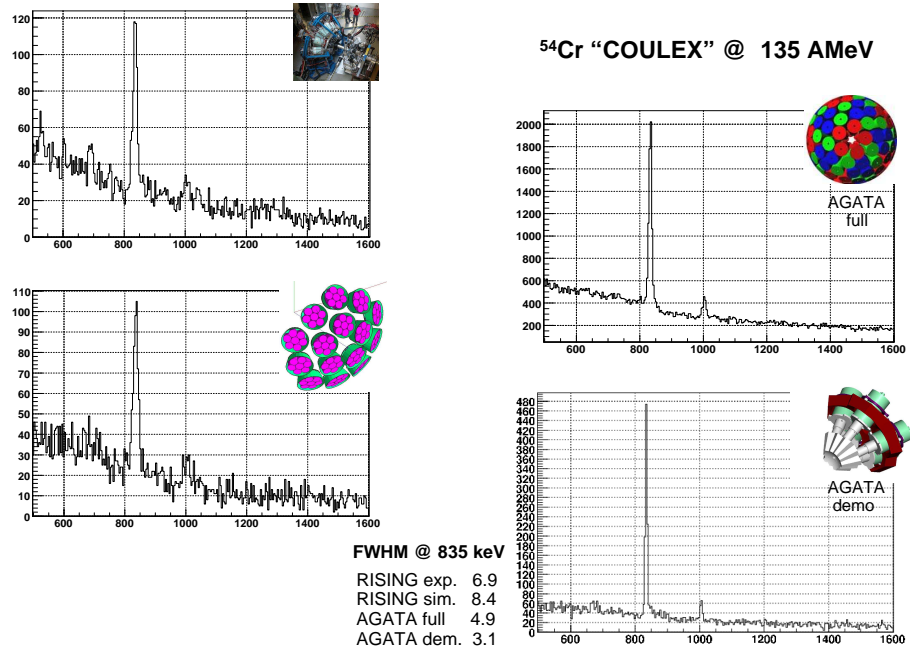


Figure A4.6. Fast beam Coulomb excitation of ^{54}Cr . Left side: experimental [A13] (upper) and simulated (lower graph) spectrum for the RISING array. Right side: the same experiment simulated with AGATA (full and demonstrator configurations) (courtesy of A. Bürger).

Another simulated example is given in Figure A4.6, which shows a comparison of

AGATA with the RISING array, for an experiment of Coulomb excitation with fast beam: the case of ^{54}Cr at 135 A MeV [A13]. The simulation of the RISING array (fifteen 7-element clusters) compares very well with the actual measurements (the left side graphs). The right side graph shows the same experiment simulated with AGATA, both in the full and demonstrator configurations. One remarks both the excellent resolution and increased efficiency in the later case.

The next example compares the AGATA demonstrator with the CLARA array, which consisted of 23 Compton suppressed Clover detectors. In both cases the γ -spectrometers are coupled to the large acceptance magnetic spectrometer PRISMA, and the experiments aim at the determination of lifetimes of nuclear states by using the RDDS (Recoil Distance Doppler Shift) method. However, in this experiment the detectors placed around 90° could not be used because in their case the Doppler shift is close to zero. Therefore, the number of useful Clover detectors was 12, with a total photopeak efficiency of the order of 1.2%. The experiment, performed at Legnaro with the CLARA array, allowed to measure, among others, the lifetime of the 2_1^+ state in ^{50}Ca with the recoil distance Doppler shift (RDDS) method. The ^{50}Ca nuclei were produced in a multi-nucleon transfer reaction of a 310 MeV ^{48}Ca beam which bombarded a target-degrader setup. The target consisted of 1.0 mg/cm^2 of enriched ^{208}Pb evaporated onto a 1.0 mg/cm^2 Ta support to accomplish the stretching of the target. A thick 4 mg/cm^2 ^{nat}Mg foil used as an energy degrader of the recoiling ejectiles was positioned after the target at accurately known distances. The reaction products passing through the degrader foil were analyzed by the PRISMA spectrometer placed at the grazing angle $\theta_{LAB} = 49^\circ$. The velocities of the recoils after the target and degrader were about 10% and 8%, respectively. Figure A4.7 shows a comparison of the

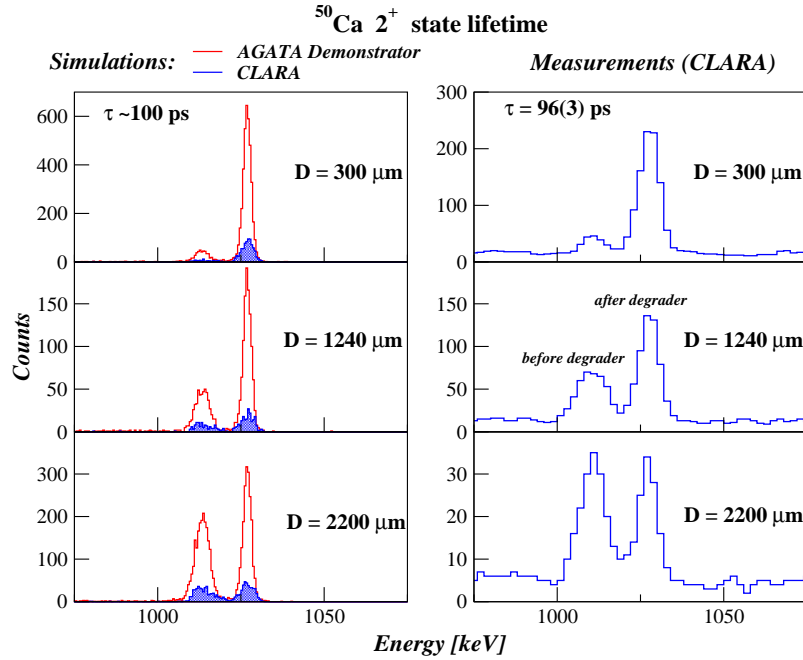


Figure A4.7. Doppler-corrected γ -ray spectra showing the $2^+ \rightarrow 0^+$ transition of ^{50}Ca in the RDDS measurements. The right spectra show the real measurement performed with the CLARA-PRISMA setup. The left spectra are simulations, and show a comparison of the AGATA demonstrator with the CLARA spectrometer. (courtesy of D. Mengoni; to be published).

measured spectra with the spectra simulated by using realistic velocity distributions after performing the Doppler correction. The AGATA demonstrator is clearly superior in both energy resolution and efficiency.

More details of other simulations of AGATA can be found in E. Farnea et al. [A14].

References

- [A1] AGATA Technical Proposal, ed. by J. Gerl and W. Korten, 2001; www-w2k.gsi.de/agata and <http://www.agata.org/reports/AGATA-Technical-Proposal.pdf>)
- [A2] J. Simpson and R. Krücken, Nuclear Physics News **13 No. 4**, 15 (2003)
- [A3] J. Simpson, J. Phys. G:Nucl. Phys. **31**, S1801 (2005)
- [A4] J. Eberth and J. Simpson, Prog. Part. Nucl. Phys. **60** (2008) 283
- [A5] E. Farnea *et al.*, LNL Annual Report 2003, LNL-INFN(REP)-202/2004, 160.
- [A6] E. Farnea, <http://agata.pd.infn.it/documents/simulations/comparison.html>
- [A7] D. Bazzacco, private communication.
- [A8] A. Lopez-Martens *et al.* Nucl. Inst. Meth. **A533**(2004) 454.
- [A9] D. Bazzacco, Proc. Workshop on Large γ -ray Detector Arrays, Chalk River, Canada, AECL-10613, p. 376
- [A10] C. Rossi Alvarez, Nucl. Phys. News. 3(3) (1993)
- [A11] A. Gadea *et al.*, J. Phys. G: Nucl. Part. Phys. **31** 92005) S1443
- [A12] J. Simpson et al., APH N.S. Heavy Ion Phys. **11** (2000) 159.
- [A13] A. Bürger *et al.*, Phys. Lett. B622(2005)29.
- [A14] E. Farnea *et al.*, Proceedings of the 2008 Zakopane Conference on Nuclear Physics (to be published in Acta Physica Polonica **B**).